THESIS FOR THE DEGREE OF LICENTIATE OF ENGINEERING

Tellurium Behavior and Management in the Liquid Phases in the Containment During a Severe Nuclear Reactor Accident

ANNA-ELINA PASI

Department of Chemistry and Chemical Engineering

CHALMERS UNIVERSITY OF TECHNOLOGY

Gothenburg, Sweden 2020

Tellurium Behavior and Management in the Liquid Phases in the Containment During a Severe Nuclear Reactor Accident

ANNA-ELINA PASI

Cover:
Graphical presentation of the main findings from publication I.

I

ABSTRACT

No industry is immune to accidents; however, the consequences and the probability are the parameters to consider when assessing the risks. When considering nuclear power, two of the highest-level accidents have occurred during the course of the commercial use of nuclear energy. The consequences of these events were the release of radioactive material to the environment and increased radiation dose to the people. Severe nuclear accident research is therefore crucial in both minimizing the consequences and assessing the effects of the potential releases. The lessons learned from previous nuclear reactor accidents have resulted in higher safety standards, more accurate source term assessment, and improvements in accident management actions. Yet, there are still uncertainties about the behavior of radionuclides during a severe nuclear reactor accident that need to be addressed.

One of the elements released in a severe reactor accident is tellurium. It has several radioactive isotopes that can potentially cause an increased dose in the population if released. Moreover, many of the tellurium isotopes decay to iodine and therefore contribute to the iodine source term. The behavior and release of tellurium have been investigated in the fuel and the reactor system during the past decades. However, the released species, including tellurium, are subjected to different management actions after entering the containment including the containment spray system. The removal efficiency of the spray system towards tellurium species formed under various conditions has been unclear. In this work, the effectiveness was investigated in relation to tellurium species under various atmospheres and in the presence of cesium iodide. In addition, the effect of the chemical composition of the spray was also examined. The spray system was found to be relatively effective in all conditions tested. Moreover, the increase in chemical content of the spray solution increased the removal efficiency.

After being removed from the containment atmosphere, the species, including various tellurium compounds, may enter the containment sump. Due to the complex chemistry of tellurium, it is difficult to predict the behavior under different redox conditions and especially under irradiation. This work therefore investigated the behavior of tellurium dioxide was investigated in simplified containment sump conditions in relation to dissolution, redox reactions and interactions with water radiolysis products. The results indicate that radiolysis products have a significant effect on tellurium chemistry in both reducing and oxidizing manner depending on the solution composition. The redox reactions also affect the solubility of tellurium both by increasing and decreasing it depending on the prevailing conditions. The results show that the current information used to assess tellurium source term needs to be re-evaluated for both severe accident management as well as for severe accident code validation purposes.

Keywords: tellurium, severe nuclear reactor accident, fission product, source term

LIST OF PUBLICATIONS

I.   Pasi Anna-Elina, Glänneskog Henrik, Foreman Mark R. St-J., Ekberg Christian. "Tellurium Behavior in the Containment Sump: Dissolution, Redox, and Radiolysis Effects." Nuclear Technology (2020): 1–11.

Contribution: Main author, all experimental work, processing and interpretation of data

II.   Kärkelä, Teemu, Pasi Anna-Elina, Espegren Fredrik, Ekberg Christian, "Tellurium Retention by the Containment Spray System", *Manuscript*

Contribution: Part of the experimental work, part of processing and interpretation of data, co-author.

Table of Contents

1. Introduction

There are a range of sources used in the energy production sector. From fossil fuels and renewable energy sources, to nuclear power, each industry has reasons why they have earned their place in the market. Whether it is the efficient and economic production, low emissions or sustainable resourcing, each industry has had to prove their worth. However, discussions about the energy mix would not be as active as they are today if a perfect energy source actually existed. With nuclear power, the main advantages include reliable production, low emissions and low fuel cost. For these reasons, nuclear power has been one of the larger energy contributors since the 1960s[1]. However, one major drawback that has affected the nuclear industry as a whole is severe nuclear reactor accidents that have occurred in the past. These accidents resulted in higher safety standards but have also tainted public opinion towards the nuclear industry, leading to controversy about the safety of nuclear energy.

While no industry is immune to accidents; however, the consequences and the probability are the parameters that must be considered when assessing the risks. One of the worst examples of energy production-related accidents is the Banqiao dam failure in China in 1975. It caused 171 000 fatalities and destroyed the homes of 11 million people making it the worst technical disaster in terms of casualties[2]. In the worst-case scenario nuclear reactor accident, the consequences include releases of radioactive material to the environment. Secondary consequences of this can be the loss of human lives due to increased dose of radiation. Comparing the worst nuclear event, the Chernobyl accident, to the Banqiao dam break, the death toll is far from that. Fatalities due to acute radiation sickness caused by high dose of radiation amounted to 31[3] and the number of cancer-related deaths is estimated to be around 4000[4]. Furthermore, evacuation due to a nuclear reactor accident can also cause severe health effects, such as phycological distress and post-traumatic stress[5]. Nevertheless, the overall accident mortality differs depending on the estimates of cancer-related deaths caused by elevated dose received during and after a nuclear accident. Statistically, however, nuclear power has the lowest mortality per kWh produced considering both deaths from accidents and pollution-related deaths[6]. It has also been suggested that replacing fossil fuels with nuclear power would actually prevent mortality as well as decrease the overall greenhouse gas emissions[7]. History has shown that nuclear power plant accidents can have extremely harmful and long-lasting consequences. Research towards better accident management and accurate assessment of the timing and the amount of the releases, the source term, is therefore crucial.

The main concern during a nuclear reactor accident is the release of radioactive material to the environment. First to escape the reactor core are the fission products with highest volatility. These fission products include noble gases, iodine, cesium and tellurium Previous research efforts have focused on studying mostly iodine due to its high radiotoxicity and accumulation in the thyroid gland causing an increased risk of thyroid cancer[8]. In contrast, tellurium isotopes, a proxy to some important iodine isotopes, have received less attention in severe accident

research. Moreover, several tellurium isotopes have been released in significant activities in the previous nuclear reactor accidents. Although there has been research relating to tellurium behavior during a nuclear reactor accident, there are still significant uncertainties in the tellurium source-term assessment. In particular, the behavior of different tellurium species after entering the containment as well as the potential reactions of precipitated or dissolved tellurium species in the sump remain unclear. This work aims to provide information on the management of tellurium species by the containment spray system and to assess the behavior of tellurium dioxide in the containment sump under irradiation.

2. Background

2.1. Severe accidents

The severity of radiological incidents and accidents can be assessed by using the International Nuclear and Radiological Event Scale (INES) introduced by the International Atomic Energy Agency in 1990[9]. This 7- step scale classifies the events by assessing three main areas: impact on people and the environment, impact on radiological barriers and impact on defense-in-depth. The first three levels on the scale are considered incidents, whereas levels 4-7 are classified as accidents. The schematic of the scale is presented in Figure 1, where the colors indicate the significance of the event and the greyscale the probability of occurrence. As presented, the incidence of accidents of the higher levels is significantly lower than those of the lower levels. It should be noted that the proportions only represent the trend, not the actual ratio of the incidence of the events. The scale also includes so-called level zero, which considers deviations that do not cause any safety significance.
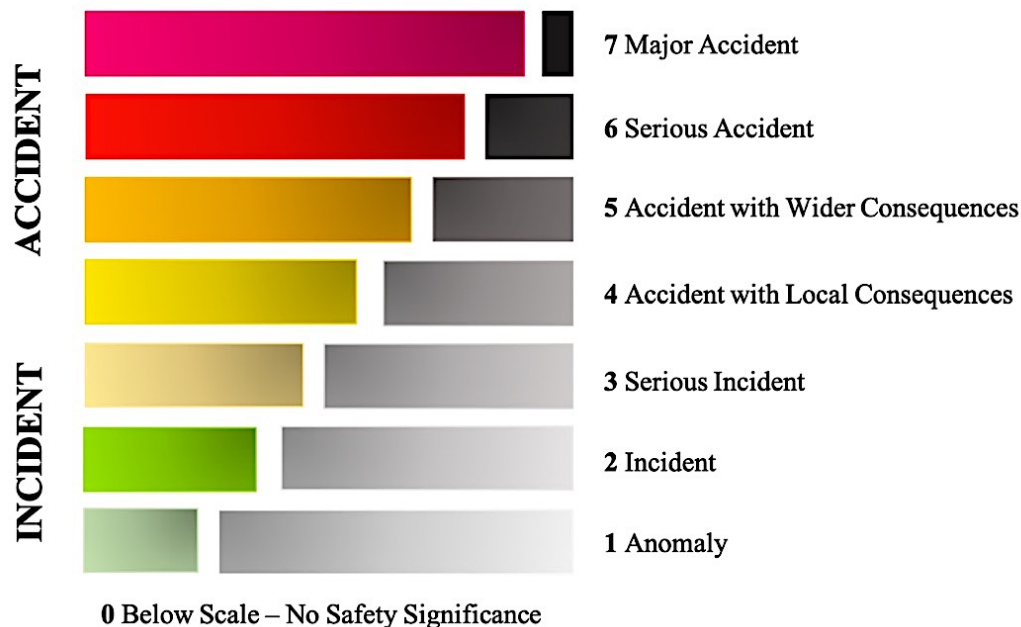
ACCIDENT

7 Major Accident

6 Serious Accident

5 Accident with Wider Consequences

4 Accident with Local Consequences

INCIDENT

3 Serious Incident

2 Incident

1 Anomaly

0 Below Scale – No Safety Significance

Figure 1. Schematic presentation of the INES scale of radiological events.

The first major accident was the Chernobyl accident in 1986, while the second one took place in the Fukushima Daiichi power plant in 2011. Both accidents included unexpected events that consequently resulted in significant releases of radioactive material to the environment. Brief descriptions of both major accidents are presented in Sections 2.1.1 and 2.1.2 Although both accidents resulted in high releases of radioactive material into the environment, the releases during the Chernobyl accident were significantly higher compared to the Fukushima releases.

This was due to differences in the reactor type and accident progression. The releases of some of the more significant radionuclides released in both major accidents are presented in Table 1. As seen in the table, the releases are of peta becquerel (10^{15} s^{-1}) magnitude and more, and the highest activities released are those of the volatile fission products (noble gases, iodine, tellurium and cesium in both reactor accidents.

Table 1. The releases of significant fission products from the Chernobyl and Fukushima accidents.

Radionuclide	Half-life[10]	Chernobyl, PBq	Fukushima, PBq
Volatile elements			
^{133}Xe	5.25 d	6500[11]	14 000[12]
^{131}I	8.03 d	1760[13]	150[14]
^{132}Te	33.6 d	1150[13]	180[15]
^{129m}Te	3.20 d	240[11]	15[15]
^{137}Cs	30.1 y	85[13]	12[14]
Intermediate volatility elements			
^{89}Sr	50.5 d	115[13]	0.2[15]
Refractory elements			
^{239}Pu	24 110 y	0.013[13]	-

2.1.1. The Chernobyl accident

The Chernobyl accident is a known example of a Reactivity Initiated Accident (RIA)[16]. RIA is caused by an unwanted increase in the fission rate and reactor power that can lead to severe core damage and disruption of the reactor operation[16]. This happened in the Chernobyl unit 4 reactor in April 1986 in the Ukrainian SSR. The Chernobyl reactor was a graphite moderated channel type reactor (RBMK) unlike most of the commercialized nuclear reactors today which are moderated and cooled by light water. The reactor design played an important role in terms of accident type and progression. For example, the RBMK type reactor had a positive reactivity feedback due to the combination of light water coolant and graphite moderator, which caused the reactor power to increase with increasing fuel and coolant temperature. Moreover, the reactor at Chernobyl also lacked a containment building which is one of the main barriers for fission product releases in today's conventional reactors[17]. Finally, the graphite used as the moderator in the RBMK reactor is very flammable and during the Chernobyl accident the graphite ignited and burned for several days causing significant releases of radioactive material into the environment. In addition to the reactor characteristics, the operator actions contributed to the devastating events. The Chernobyl accident was initiated by a reactor test in which safety guidelines were ignored, and the existing safety systems had been made ineffective[16].

As shown in Table 1, there was a significant number of radionuclides released during the Chernobyl accident. The highest activities, excluding noble gases, were those of iodine-131 and tellurium-132, 1760 and 1150 PBq, respectively. In addition, there were also direct releases from the reactor core due to steam explosions that resulted in releases of core and structural

materials. Consequently, some low and non-volatile elements like strontium and plutonium were released to the environment[18]. The radioactive plume released to the atmosphere was transported all over the world, across Asia to Japan[19], the North Pacific and the West Coast North America[20]. Many fission products including tellurium and ruthenium were detected in monitoring stations all over the world after the accident[21–23]. Moreover, the effects are still measurable in environmental samples especially in the Nordic countries due to high amount of deposition of long-lived radionuclides during the Chernobyl accident [24,25].

2.1.2. The Fukushima accident

The Fukushima accident was a Loss of Coolant Accident (LOCA) that was a result of a Stationary Black Out (SBO) caused by a large tsunami covering the power plant area. The events leading to the SBO started through the loss of off-site power (LOOP) due to an earthquake, after which the emergency diesel generators were started. The LOOP was within the design basis of the Fukushima reactors. Following the earthquake, a tsunami covered the plant area, causing the loss of all AC power and consequently, the start of the SBO. Later, the DC power was also lost in the plant area. The units in Fukushima were designed to withstand an SBO for eight hours with DC power supply, however, due to the loss of all power caused the accident to progress[26]. Although, the reactors had responded to the earthquake as they were designed to, and all of the control rods had been inserted, the core of a nuclear reactor requires cooling due to remaining decay heat produced by the fission products. The loss of all off and on-site power resulted in the loss of cooling capability, leading to the LOCA situation. Consequently, the water in the reactor started boiling, which resulted in the uncovering and partial melting of the fuel. This led to the release of radionuclides into the reactor building and further on to the environment. The general fission product release phases are discussed in more detail in Section 3.1.

As a result of the Fukushima accident, large amounts of radionuclides were released to the environment. The distribution and deposition of the radionuclides were monitored by measuring environmental samples[27,28] as well as air filters[29] during the release period. In addition, different modelling tools were used to estimate the deposition of radionuclides in air and water after the accident[30,31]. Most of the terrestrial deposition was to the north-west from the plant. It is estimated that 70-80 % of the overall atmospheric releases during the accident was deposited to the Pacific Ocean due to the east-blowing wind during the release plumes[32]. Using the deposition models for individual radionuclides, it is possible to tie the releases to the plant events and therefore estimate the possible source term of the radionuclide releases.

The deposition of fission products (e.g. $^{134,\ 137}$Cs, ^{131}I, ^{129m,132}Te), was monitored during the Fukushima accident as well as later from soil samples[33–35] and through simulations[36]. As mentioned, the highest deposition of radionuclides was to the northwest of the power plant for all of the fission products. However, in terms of areal distribution, there seem to have been some differences between the behavior of tellurium and iodine compared to cesium, which

raises uncertainties concerning the behavior of these nuclides during the Fukushima accident. By comparing the isotopic ratios of radionuclides, it is possible to estimate the release behavior or the behavior in the environment. After the Fukushima accident, ^{131}I/^{137}Cs and ^{129m}Te/^{137}Cs ratios were compared and it was found that both ratios were higher to the south of Fukushima than to the northwest.[35] This might indicate differences in timing of the release or in the transport behavior. On the other hand, ^{129m}Te/^{137}Cs ratios were more consistent compared to ^{131}I/^{137}Cs indicating greater differences in iodine transport behavior. Nevertheless, this raises uncertainties in terms of the source term of tellurium during an accident, and whether the timing and pathway of the releases are accurately known. The deposition of ^{131}I and ^{129m}Te in Japan after the Fukushima accident is presented in Figure 2. It should be noted that ^{129m}Te is often used to also estimate the deposition of the short-lived ^{132}Te due to their analogous behavior.
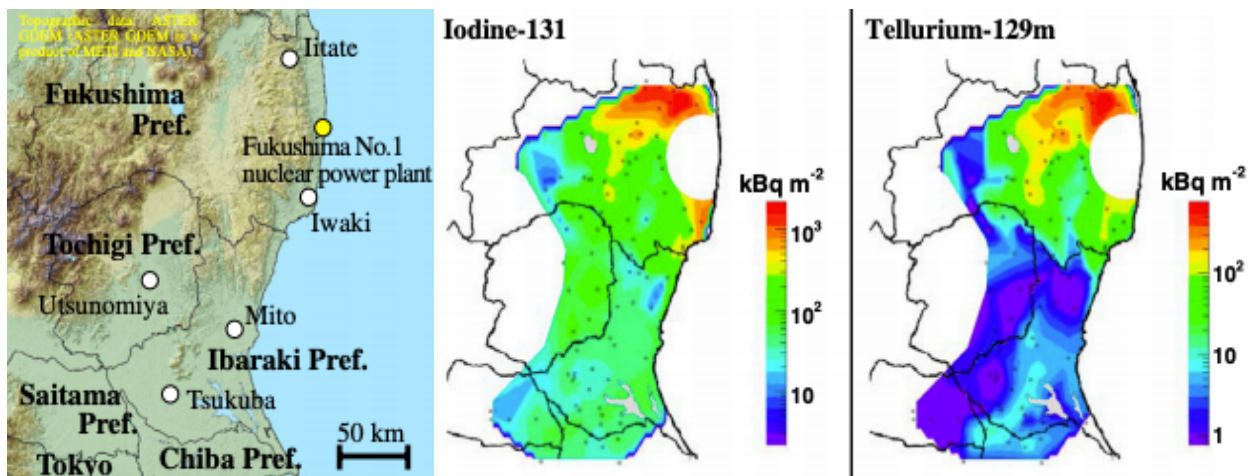

Figure 2. The distribution of iodine-131 and tellurium-129m after the Fukushima accident in Japan[34].

2.2. Tellurium in severe accident scenarios

As presented earlier, the majority of the releases from a nuclear reactor accident are the fission products with the highest volatility. The main focus in terms of severe nuclear accident research has been on iodine and cesium releases due to their radiotoxicity and sufficiently long half-lives. As one of the volatile fission products, tellurium should also be considered significant in safety assessments due to the relatively the long half-lives of the released tellurium isotopes. Furthermore, some of the tellurium isotopes decay to iodine and so the significance of the potential tellurium releases is great. Even though iodine has received more attention in terms of severe accident research, it should be noted that tellurium is still considered radiologically significant. According to the radiological equivalence data from the International Atomic Energy Agency (IAEA), tellurium-132 has a multiplication factor of 0.3 in a scale normalized to ^{131}I[9]. Although, the equivalence of ^{132}Te is lower, due to the volatility resulting in potentially

high releases, the significance is justified. The main tellurium isotopes in severe nuclear reactor accident scenario, are presented in Table 2 along with their decay products and half-lives.

Table 2. Relevant tellurium isotopes, their half-lives, combined core inventories in Fukushima units 1–3, and daughter isotopes.

Te isotope	Half-life[10]	Core inventory of Fukushima units 1-3[37]	Decay product	Decay product half-life
^{127m}Te	109 d	3.36×10^{16}	^{127}I	stable
^{129m}Te	33.6 d	1.89×10^{17}	^{129}I	1.57×10^{7}
^{131m}Te	30 h	1.38×10^{18}	^{131}I	8.02 d
^{132}Te	3.2 d	8.68×10^{18}	^{132}I	2.295 h
^{133m}Te	55.4 min	6.06×10^{18}	^{133}I	20.8 h
^{134}Te	41.8 min	1.14×10^{19}	^{134}I	52.5 min

Previous research efforts related to tellurium behavior have been focused on the release from the fuel [38,39], interactions with the cladding [40,41], transport in the reactor coolant system (RCS)[42,43] and the species entering the containment [44]. However, once tellurium species enter the containment and are subjected to severe accident management actions and pass further on to the aqueous phases, the data becomes relatively scarce. Due to the complex chemistry and possibilities in appearing as various species depending on the prevailing conditions, tellurium behavior is difficult to predict. Experimental data is therefore necessary to determine the tellurium behavior throughout the whole accident progression in order to estimate the tellurium source term.

2.3. Release of fission products

Before released to the environment, the fission products need to pass several barriers and containment levels; beginning with the fuel matrix and cladding, continuing on to the reactor vessel and finally the last barrier, the containment building. The release pathways can be divided into two phases – the in-vessel phase and ex-vessel phase. These are schematically presented in Figure 3. The in-vessel phase is initiated when fuel degradation begins, and the geometry of the core is lost. In this phase, the most volatile elements, such as noble gases, iodine, cesium and tellurium, are released into the reactor coolant system (RCS).[45] Some of the more volatile fission products interact with materials found in the RCS that affect the amount released. Generally, the residence times in the RCS are longer in a high-pressure accident sequence, resulting in high retention. Conversely, the retention is lower in a low-pressure sequence and the release to the containment is higher [46]. If the accident progresses to the point where the Reactor Pressure Vessel (RPV) fails and the molten corium comes in contact with the concrete, additional releases can occur. The Molten Corium Concrete Interactions (MCCIs) produce gases, such as CO and CO_2 [47], that can affect the release of fission products. As a result of the MCCIs, less volatile elements, like strontium and barium, can be released through vaporization[48]. Whether the release is through the RCS or via vessel failure and MCCI interaction, the species enter the containment. One exception is the containment bypass, where the species are released into the environment without entering the containment building[45].
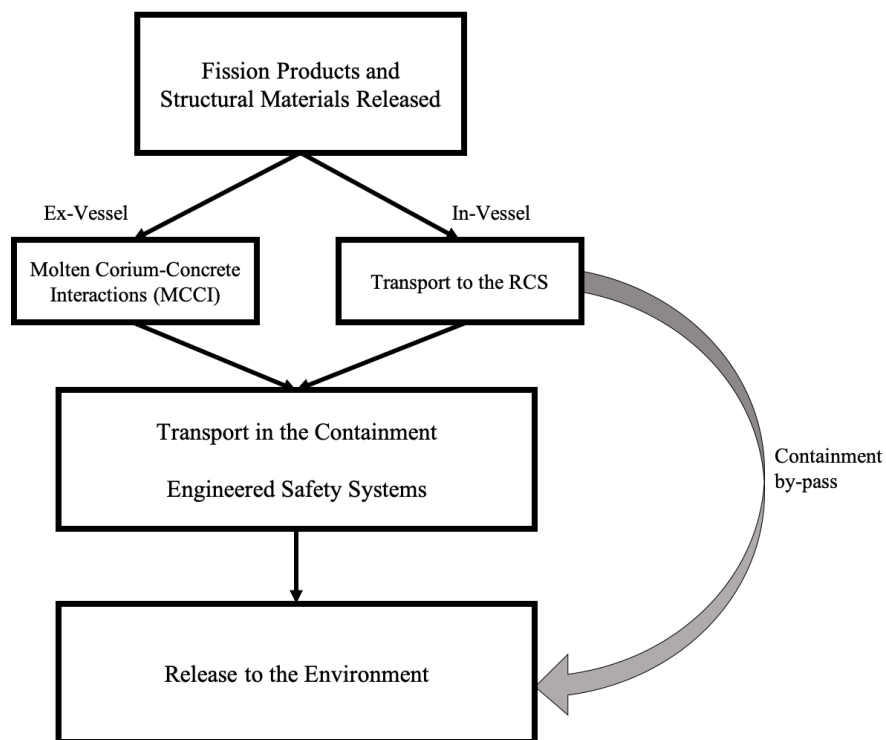

Figure 3. Schematic of the different release phases. Reproduced from Ref [45].

8

2.4. Severe accident management

The following sections present a brief introduction to severe accident management principles as well as some of the management actions relevant for this work. The focus is on the containment spray system and the related chemistry as well as the main components and phenomena related to the containment sump.

The most important consideration for nuclear power production is the plant safety. Preparedness against unlikely incidents and accidents is covered by various plant-specific guidelines. In the event of an unexpected incident or accident, Emergency Operation Procedures (EOPs) are applied. The EOPs have been developed to guide the operators to respond to Design Basis Accidents (DBA) as well as, to some extent, incidents that go beyond the design basis accident (BDBA) sequence. The main aim of the EOPs is to reach a final stable state of the core. In an event where an accident proceeds beyond the limits of the EOPs and the core integrity is lost, the operators need to apply guidelines designed for severe accident events. The Severe Accident Management Guidelines (SAMGs) are applied in a situation where the core integrity has already been compromised.[45] Thus, the main objective of the SAMGs is to minimize the radioactive releases by protecting any of the fission product boundaries. The SAMGs may not prevent large releases but they can delay and reduce the releases so that the emergency organizations have more time to protect the general public and implement protective actions. Moreover, the SAMGs vary according to the plant design and local regulations but in general the end goals are generally the same. Both emergency response actions and their main objectives are presented in Figure 4[49]. As shown, the dividing factor between the use of EOPs and SAMGs is the core damage. However, there are overlapping features between the use, and in some operating procedures the maximum set point for EOP can be the initiating point for the application of the SAMG.
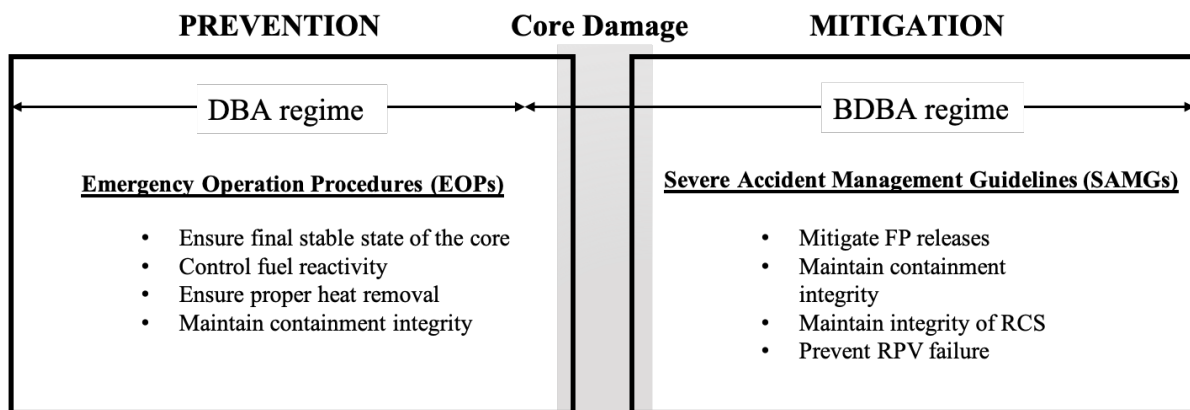

PREVENTION   **Core Damage**   **MITIGATION**

DBA regime	BDBA regime
Emergency Operation Procedures (EOPs)	**Severe Accident Management Guidelines (SAMGs)**
• Ensure final stable state of the core • Control fuel reactivity • Ensure proper heat removal • Maintain containment integrity	• Mitigate FP releases • Maintain containment integrity • Maintain integrity of RCS • Prevent RPV failure

Figure 4. The main objectives of the Emergency Operation Procedures and Severe Accident Management guidelines.

9

3. Theory

3.1. Containment spray system

The containment spray system (CSS) is one of the engineered safety systems designed for severe accident management. It serves for several purposes; it maintains the containment building integrity by decreasing the pressure inside the containment, it mitigates the release of radionuclides by removing the fission product containing particles from the containment atmosphere into the sump and it helps maintain the sump pH at the desired value. The CSS has been found to be efficient at removing aerosols as well as some gaseous compounds. Gaseous species can be removed by adjusting the chemistry of the spray solution to react with the gaseous compounds and converting them into a non-volatile form [50].

The removal of aerosols can be explained by using basic aerosol physics. For aerosol particles, the removal efficiency is strongly related to the particle size. For larger particles, the most effective removal happens through sweep-out and interception, as the aerosols have sufficient inertia and collide to the surface of the droplet rather than following the streamline around it. The smaller particles are removed through diffusion to the droplet surface [45]. The removal efficiency has been found to be the most efficient for particles larger than 1 μm or smaller than 0.1 μm [51]. The schematics of the main aerosol removal processes are presented in Figure 5 where the largest sphere represents a falling spray droplet and the smaller spheres represent the different sized aerosol particles and their interactions with the droplet.
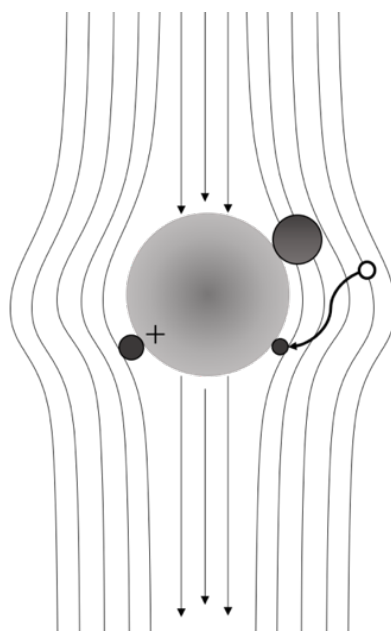
Figure 5. Interactions between a droplet and aerosol particles of different size. The largest sphere represents a falling droplet and the smaller spheres represent different size aerosols and their interactions; interception, electrophoresis and diffusion.

The chemical composition of the spray solution is primarily designed to mitigate both particulate and gaseous iodine species[52]. Moreover, the main components of the CSS solution are a base (e.g. sodium hydroxide, potassium hydroxide or trisodium phosphate), boric acid, and in some plant designs, an additive (e.g. sodium thiosulfate, hydrazine). The spray solution pH is generally kept alkaline to shift the disproportionation of volatile iodine to a non-volatile iodate/iodide side[53]. Similarly, the use of additives, usually reducing agents, reduce the amount of volatile iodine species by decomposing and trapping the gaseous species inside the droplets [54,55]. The decomposition is especially important in removal of organic iodides[55]. Finally, boric acid is used to maintain the subcriticality of the reactor core as well as buffer the pH with the base[53]. As mentioned earlier, the spray solution ends up at the bottom of the containment and forms a major part of the sump. Thus, the chemistry of the spray solution is also important when considering reactions taking place in the sump.

3.2. Containment sump

The containment sump is a complex mixture of components originating either from accident management systems e.g. the CSS or from events that take place during the accident e.g. leaks from the primary circuit, radiolysis of structural materials, water and air and corrosion and dissolution of materials from the surfaces[56]. Potential components present in the containment sump are presented in Table 3 along with their sources. Due to the complexity of the sump, it is difficult to predict the behavior of fission products and possible reactions leading to releases through re-volatilization. However, this must be considered since the sump formed during an accident will stay inside the containment and could be subjected to further chemical effects[57].

Table 3. Main components in the containment sump during a severe accident[56,58].

Source	Component
Cooling water (CSS, Safety Injection System (SIS), Emergency Core Cooling System (ECCS))	B, Li, Na, Cl, organic material
pH adjustment	sodium triphosphate (TSP), sodium hydroxide (NaOH), sodium tetraborate (NaTB)
Spray additives	Sodium thiosulfate ($Na_2S_2O_3$), hydrazine (N_2H_4)
Insulation material (e.g. fiberglass, calcium silicate)	Si, Al, Ca, Mg, B
Concrete	Si, Ca, Al
Metals, steel, coatings	Al, Zn, Fe, Ni, S, Cu

The pH of the containment sump is targeted to stay above 7 in accident, conditions which is done by adding base in the alkaline spray solution for pH management[58]. More precisely, the target pH is generally around 9.3[59]. The pH is maintained alkaline in order to keep iodine as a soluble species and thus minimize the possible iodine re-volatilization from the sump back into the containment atmosphere. However, the radiolysis and pyrolysis of air and cables produce hydrochloric and nitric acid, respectively, which can lower the pH of the sump during the accident[60]. In addition, reactions of different fission products, including tellurium[61,62], with organic compounds originating from paint, ion exchange resins or insulation materials in the sump can lead to more volatile species and increase the source term[63,64].

3.2.1. Water radiolysis

In addition to the substances already mentioned, the splitting of water molecules into reactive species due to ionizing radiation from fission product decay needs to be considered. The radiolysis of water produces both oxidizing ($\bullet OH$, H_2O_2) and reducing (e^-, $H\bullet$) species[65] that can quickly react with fission products present in the sump. The change in speciation of fission products is especially important because change in oxidation state can have a significant effect on the volatility of a fission product. This might consequently result in higher amounts of volatile fission products and possibly higher environmental releases. The production of primary radiolysis products and their respective G-values (µmol/L) in natural water produced by a low linear energy particle (X-ray, gamma or electron) are presented in Equation 1[66].

$$H_2O \rightarrow [0.28] \cdot OH + [0.07]H_2O_2 + [0.05]H_2 + [0.27]H_3O^+ + [0.27]e_{aq}^- + [0.06]H^{\cdot} \quad (1)$$
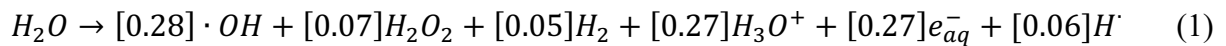
The extent of radical and molecular product formation is highly dependent on the Linear Energy Transfer (LET) of the type of radiation. High LET radiation (alpha) is strongly ionizing and has a short range in water and hence, deposits its energy more locally than low LET radiation (Gamma, beta, x-ray). The local production of radicals leads to recombination and production of more molecular species rather than radicals.[67]

Radiolysis becomes even more complex when pH, scavenging agents and dissolved oxygen are taken into account. In acidic and alkaline solutions there are H^+ or OH^- ions, respectively, that can react quickly with the initial radiolysis products before they diffuse from the spur. According to literature there seems to be no significant effect on the rate and extent of primary radiolysis product produced in a narrow pH range. However, the pH effects become considerable at extreme pH values when the H^+/OH^- concentration increase[68]. In acidic solution, solvated electrons, e^-_{aq}, are consumed by H^+ ions (Equation 2). Conversely, OH^- ions present in an alkaline solution react with radiation produced H_3O^+ and also convert •OH into O• (Equation 3)[69].

$$e^-_{aq} + H^+ \rightarrow H^. \tag{2}$$

$$HO^. + OH^- \rightarrow O^{.-} + H_2O \tag{3}$$

3.3. The chemistry of tellurium

In this work, tellurium is considered important for its radioactive isotopes and for the risk of the general public receiving increased radiation dose due to the release of tellurium. However, whether the interest in on the radioactive or the stable tellurium isotopes, the chemistry can be considered mostly analogous. The following sections therefore focus on the general chemistry of tellurium and the parameters relevant for this work e.g. solubility and redox reactions.

Tellurium is part of the chalcogen group alongside selenium and polonium. It adopts both metallic and non-metallic properties and is therefore characterized as a metalloid. Moreover, the metalloid nature gives tellurium a metallic appearance but a brittle nature and low electrical conductivity. Due to its metalloid properties, tellurium is used to improve machinability in steel alloys and as a semiconductor in CdTe solar panels. In the environment, tellurium is found in very low concentrations, only a few µg per kg. In the bedrock, tellurium is often associated with gold tellurides such as calaverite and krennerite, both polymorphs of $AuTe_2$ [70].

In aqueous solution, tellurium speciation is highly dependent on redox and pH conditions[71]. Tellurium can exist in oxidation states between -2 and +6, of which +4 and +6 are the most abundant in natural waters[70]. Solid elemental tellurium is stable in water or aqueous solution but not in extremely alkaline solution (pH>10) or in the presence of an oxidizing agent. If elemental tellurium is brought to an aerated solution, it is covered by tellurium dioxide, TeO_2[72] as could happen in sump conditions. TeO_2 is an amphoteric compound and thus can act as an acid or a base depending on the prevailing conditions. The dominant Te(IV) species in neutral aqueous solution is tellurous(IV) acid H_2TeO_3, which, depending on the pH, can undergo either protonation to form a cationic product or deprotonation, to form anionic products. The solubility of TeO_2 is relatively low, with a minimum at around 2.1×10^{-10} mol/dm^3 at pH 5.5[73].

However, the solubility increases in both extremes of the pH scale when TeO_2 dissolves as an ionic species. This is a result of the amphoteric nature of TeO_2. In a hydrated form, $TeO_2 \cdot H_2O$, the solubility increases significantly and reaches a maximum at 1.6×10^{-2} mol/dm³ in alkaline solution.[73]

Elemental tellurium can undergo reduction or oxidation reactions to form either Te^{2-} or Te(VI), respectively. The speciation of tellurium in various Eh and pH conditions is presented in Figure 6 as a Pourbaix diagram[73]. The diagram presents the equilibrium phases in an aqueous electrochemical system as a function of potential and pH. For tellurium, both the elemental form and TeO_2 are the dominating stable solid phases. It can be seen from the diagram that, in higher oxygen potentials, tellurium is in a form of Te(VI) species. The Te(VI) aqueous species is telluric acid, which can undergo protonation or deprotonation. In reducing conditions, Te is present as Te^{2-}, which can also protonate in lower pH values to form HTe^- or H_2Te. As the pH of the sump during an accident is targeted around pH 9, the interest in tellurium behavior focuses on alkaline conditions. However, local production of acids could be considered important as well. In addition, the behavior of tellurium under the whole potential scale is of interest due to water radiolysis producing both oxidizing and reducing species. The Pourbaix diagram is useful in estimating the speciation of an element in different potential-pH conditions. However, it does not provide information about the kinetics of the reactions from one species to another.
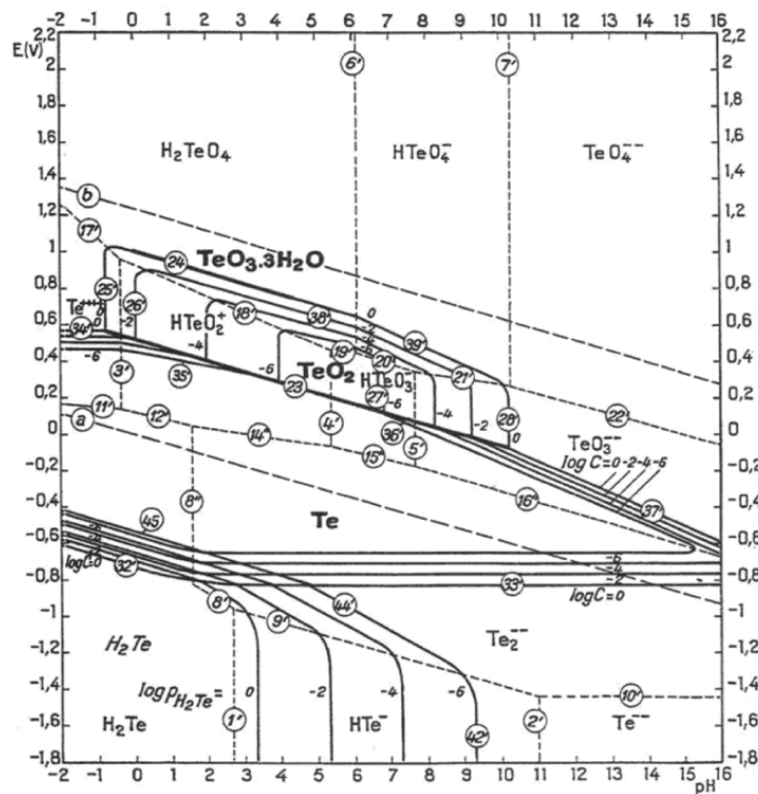

Figure 6. Pourbaix diagram of tellurium showing Eh-pH dependency and speciation[73].

14

Due to its complex chemistry, tellurium can take part in multiple redox reactions depending on the prevailing conditions. Standard reduction potentials of several tellurium(IV) and tellurium(VI) reactions relevant to the study are presented in Table 4. The aforementioned radiolysis products can have a significant effect on tellurium redox chemistry. Different oxidizing and reducing agents can also be of importance. As mentioned earlier, most additives used in the accident management systems, e.g. sodium thiosulfate and hydrazine (N_2H_4), are designed to decompose iodine species[74]. The effect of any additive on tellurium chemistry relevant to nuclear accident scenarios has not previously been investigated. However, the effect of change in redox conditions may be relevant due to the complex chemistry of different tellurium species.

Table 4. Standard reduction potentials for possible Te(IV) and Te(VI) redox reactions[72].

$Te(IV) \leftrightarrow Te(0)$	Standard potential, V
$TeO_3^{2-} + 4e^- + 6H^+ \leftrightarrow Te(s) + 3H_2O$	+0.827
$TeO_2(s) + 4e^- + 4H^+ \leftrightarrow Te(s) + 2H_2O$	+0.521
$TeO_2aq(s) + 4e^- + 4H^+ \leftrightarrow Te(s) + 2H_2O$	+0.604
$Te(VI) \leftrightarrow Te(IV)$	
$HTeO_4^- + 2e^- + H^+ \leftrightarrow TeO_3^{2-} + H_2O$	+0.584
$H_2TeO_4 + 2H^+ + 2e^- \leftrightarrow TeO_2 + 4H_2O$	+1.020
$HTeO_4^- + 3H^+ + 2e^- \leftrightarrow TeO_2(s) + 2H_2O$	+1.202
$HTeO_4^- + 3H^+ + 2e^- \leftrightarrow TeO_2aq(s) + 2H_2O$	+1.036

3.4. Release of tellurium in severe accidents

During normal operation, the speciation and vapor pressure of tellurium is highly dependent on the chemical oxygen potential in the core[75]. Due to the excess of cesium in the core compared to tellurium, the formation of cesium telluride, Cs_2Te plausible. In high oxygen potentials, cesium is retained, and the possible speciation of tellurium is in the form of palladium telluride, PdTe. If any ternary phases form, one of the suggested species is cesium telluride, Cs_2TeO_3. However, no studies presenting the formation of it have been published. When tellurium reaches the gap between the fuel and the cladding in elemental form, it will combine with zirconium to form different zirconium tellurides e.g. $ZrTe_2$, Zr_4Te_5[40].

In severe accident scenario, tellurium is considered one of the more volatile fission products and is released in early and mid-stages of the accident. The release of tellurium from the core is highly governed by speciation, atmosphere and the degree of oxidation of the zirconium cladding[41]. Depending on the accident conditions, tellurium, can be released as elemental Te, H_2Te, SnTe, Te_xO_y or Cs_2Te [76]. Conditions and their respective tellurium species are presented in Table 5. The formation of different tellurium species and their behavior in accident conditions is discussed in more detail below.

Table 5. Gas phase tellurium species in accident conditions[76].

Species	Conditions
Te, Te$_2$, H$_2$Te	T>1400 K, steam or H$_2$/steam
Te$_x$O$_y$	Oxidizing atmosphere
Cs$_2$Te	T<1400 K, dominates over SnTe in inert atmosphere
SnTe	H$_2$/steam, air/steam

One key feature sets tellurium apart from most of the other fission products in terms of the release behavior from the core. This is the interactions between tellurium and the zirconium in the cladding. As mentioned above, elemental tellurium tends to form zirconium tellurides in the fuel-cladding gap even in normal operation. Furthermore, the interactions between zirconium and tellurium in an accident scenario result in retention of tellurium until the zirconium in the cladding is sufficiently oxidized. Consequently, tellurium releases are delayed compared to e.g. iodine and cesium, which do not interact with the cladding material.

The oxidation of the zirconium telluride resulting in the release of tellurium is presented in Reaction 4[75]. In general, if any steam or oxidants reaches the cladding at temperatures higher than 1150 K, zirconium will be oxidized. As long as the cladding is intact, tellurium will be in the form of a zirconium telluride. However, once the cladding is breached and subjected to H$_2$/H$_2$O conditions, oxidation takes place. This results in the zirconium telluride compounds dissociating, and tellurium being released in an elemental form. In very high hydrogen pressures, tellurium can form hydrogen-tellurium compounds (Reaction 5) with the most stable one being hydrogen telluride, H$_2$Te.

$$ZrTe_2(s) + 2H_2O \rightarrow ZrO_2 + 2H_2(g) + Te_2(g) \qquad (4)$$

$$2H_2(g) + Te_2(g) \rightarrow 2H_2Te(g) \qquad (5)$$
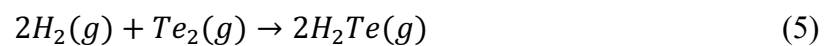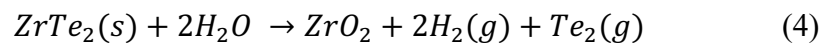
As the oxidation of the cladding progresses, tin, an alloy element in the cladding material, is mobilized. Due to its low vapor pressure and melting point, tin forms a boundary layer between the metallic non-oxidized zirconium and the already oxidized ZrO$_2$[77]. As a result of the tin-rich areas, tin-tellurium compounds can form. Tin telluride, SnTe is stable in air/steam atmosphere but has been found to vaporize as gaseous SnTe at around 1000 K[78].

Similarly to the fuel, the speciation of tellurium is also affected by the prevailing conditions in the primary heat transport system. According to thermodynamic calculations, the main parameters affecting tellurium speciation are temperature, oxygen partial pressure, amount of tellurium and humidity.

One of the species potentially present in the fuel is Cs_2Te. In the RCS in high pressures it is likely that Cs_2Te oxidizes according to Reaction 6 to produce elemental tellurium[76]. The reaction is thermodynamically favored in the RCS conditions. The effect of cesium on tellurium speciation therefore diminishes.

$$Cs_2Te(s) + 2H_2O(g) \rightarrow 2CsOH(s) + Te(s) + H_2(g) \tag{6}$$
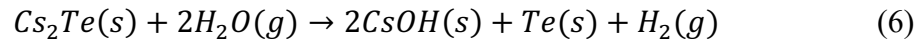
At lower temperatures of below 550 K, elemental tellurium and Te_2 dimer are the dominant species in the RCS. As the temperature increases and reaches values around 1400 K, the tellurium dimer dissociates and the most abundant species are elemental Te and tellurium monoxide, TeO[79]. However, if the tellurium concentration decreases, according to the Le Chatelier principle, the formation of tellurium oxides becomes favorable. The formation is presented in Reaction 7 and if the Te concentration decreases the equilibrium shifts to the right to produce more of the monoxide.
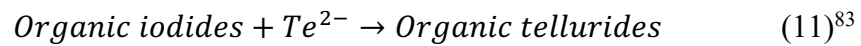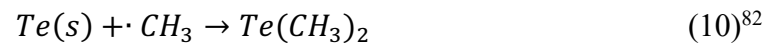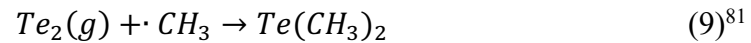
$$Te_2(g) + H_2O \rightarrow TeO\ (g) + Te + H_2 \tag{7}$$
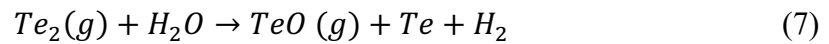
In high hydrogen concentrations, the formation of H_2Te is possible. However, it is unstable at lower temperatures and dissociates, making elemental Te the predominant species. If the H_2/Te ratio is high, H_2Te can form in significant quantities[79]. Moreover, the species is very soluble in water. Thus, H_2Te will dissolve and not be necessary for consideration if water is present in the RCS.

In highly oxidizing conditions, tellurium will further oxidize to tellurium dioxide, TeO_2. In lower temperatures TeO_2 is present as a solid whereas in temperatures above 1006 K, TeO_2 volatilizes and is present as a gaseous species. In the presence of steam, it has been observed that the volatility of TeO_2 is enhanced. The proposed reaction producing an intermediate species tellurium oxyhydroxide, $TeO(OH)_2$ is presented in Reaction 8[80]. It has been suggested that the formation of $TeO(OH)_2$ could be the reason for increased volatility of $TeO_2(s)$ in atmospheric pressures. However, no experimental evidence has yet been presented.

$$TeO_2(s) + H_2O \rightarrow TeO(OH)_2(g) \tag{8}$$
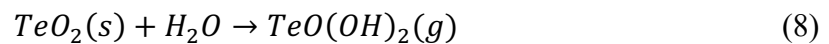
Most of the tellurium species potentially present in the RCS have very low vapor pressures in temperatures below 420 K. Thus, if any gaseous tellurium species enter the containment in gaseous form e.g. Te_2, SnTe, they will rapidly condense, and either deposit on the bottom of the containment or onto different surfaces[63].

Another possibility affecting tellurium speciation in the containment is formation of organic tellurides. The organic material originating from insulation, paint, seals or ion exchange resins, could decompose to radicals and react with tellurium in either the gas or liquid phase to form volatile organic tellurides[76,78]. Of the organic tellurides, dimethyl and diethyl tellurides are the species of interest in the context of severe accident research. Dimethyl telluride can form from reactions between tellurium and organic radicals (Reactions 9, 10) as well as from reaction between organic iodides and tellurium (Reaction 11). The organic tellurides have significantly lower boiling points compared to elemental tellurium and therefore are more volatile. However, very little research has been conducted on the role of organic tellurides in severe accidents. In addition, the possibility of organic iodide formation through the decay of tellurium in organic tellurides is something to consider.

$$Te_2(g) + \cdot CH_3 \rightarrow Te(CH_3)_2 \qquad (9)^{81}$$

$$Te(s) + \cdot CH_3 \rightarrow Te(CH_3)_2 \qquad (10)^{82}$$

$$Organic\ iodides + Te^{2-} \rightarrow Organic\ tellurides \qquad (11)^{83}$$

4. Experimental

4.2. Materials and methods

4.2.1. *Effectiveness of the spray system*

The experiments about the effectiveness of the CSS on tellurium species was done at VTT Technical Research Center of Finland Ltd. as part of a collaboration project. The aim was to investigate the efficiency of the spray system towards tellurium species formed under various conditions. The effect of the spray composition was also investigated.

The experimental spray setup consisted of a spray chamber made of stainless-steel simulating a containment building. The inner walls of the chamber were coated with Teflon tape to passivate the surfaces and thereby decrease loss of material due to adsorption. The chamber was connected to a tubular furnace (Entech/Vecstar, VCTF 3) where the tellurium precursor was vaporized. The schematics of the "VTT spray chamber" is shown in Figure 7 along with its dimensions. A spray nozzle (model Lechler 136.330.xx.16) simulating a containment spray system (CSS) was attached on top of the chamber. The spray droplets (ca. 10 μm in diameter) were generated from the solution in the spray supply bottle and the droplet feed rate was controlled with a pressurized air or nitrogen. The spray cone width was 60 mm at a distance of 150 mm from the spray nozzle, and 120 mm at a distance of 300 mm (spray angle was 20 degrees). The temperature of the spray solution and spray chamber was 293 K. The aerosol flow not captured by the spray droplets exited close to the top of the spray chamber. Downstream of this exit, the aerosol flow was diluted and dried with hot gas flow of air or nitrogen (373 K). Aerosols were filtered out after the hot dilution (at a location with a temperature of 303 K). The filter was a 47 mm polytetrafluoroethylene filter (Mitex) positioned at the end of the system. Beyond the filter, two sequential 0.1 M sodium hydroxide traps were positioned to ensure retention of any gaseous tellurium species possibly released through the setup. The spray droplets generated during the experiments were accumulated at the bottom of the chamber, forming the sump, which was collected for analysis along with the filter, trap and crucible.
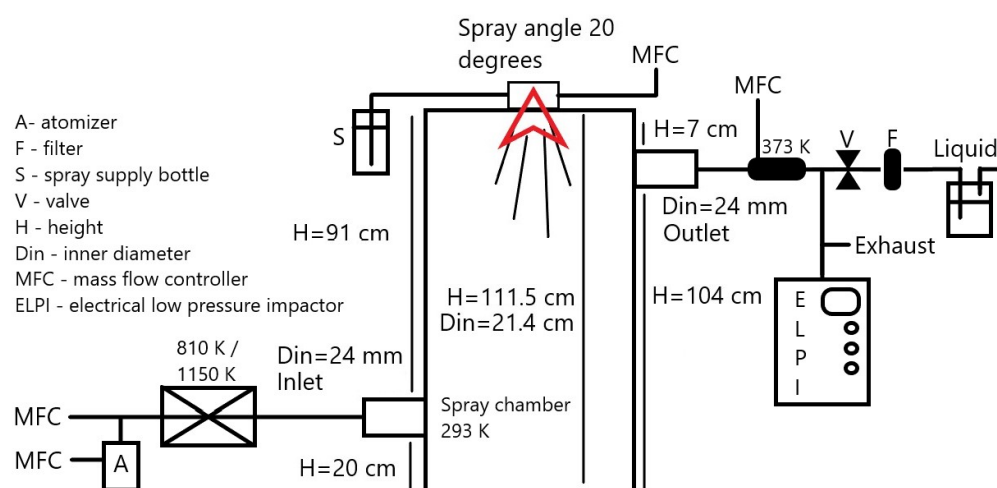
Figure 7. The experimental setup used in the spray experiments.

The experiments were performed by placing the crucible with the precursor, either Te or TeO$_2$, in the alumina tube inside the furnace. The furnace was heated close to the boiling point of the chosen precursor; 810 K for metallic Te and 1150 K for TeO$_2$. First, a reference sample was collected in order to determine how much tellurium species was generated and transported through the system when the spray was not on. After the reference sample, each solution was sprayed inside the containment unit for 20 minutes and samples were collected for analysis. Overall, nine experiments were performed in various conditions and using the two different precursors. The conditions investigated were dry and humid air and nitrogen. In addition, the effect of cesium iodide (CsI) was also investigated in both conditions by dissolving solid CsI to the water sprayed in the system via the atomizer. The sample matrix and the changing parameters are shown in Table 6. In terms of the spray solution, three were investigated – water, alkaline borate solution and alkaline borate solution with sodium thiosulfate. The concentrations of the chemicals in the solutions were 0.23 M H$_3$BO$_3$, 0.15 M NaOH, 0.064 M Na$_2$S$_2$O$_3$.

Table 6. Experimental matrix with the different parameters.

Experiment#	Precursor	Temperature, [K]	Atmosphere	Added humidity[a]	CsI[b]
1	TeO$_2$	1150	Air	No	
2	TeO$_2$	1150	Air	Yes	
3	TeO$_2$	1150	Air	Yes	Yes
4	Te	810	Air	No	
5	Te	810	Air	Yes	
6	Te	810	Air	Yes	Yes
7	Te	810	Nitrogen	No	
8	Te	810	Nitrogen	Yes	
9	Te	810	Nitrogen	Yes	Yes

[a] Humidity content of the gas flow entering the spray chamber was 21000 ppmV
[b] CsI content of the atomizer supply bottle was 0.15 M

4.2.2. Tellurium in the sump

The behavior of tellurium dioxide in the sump was investigated in terms of its solubility, speciation and reactions with water radiolysis products. Tellurium dioxide was chosen as the precursor due to its possible occurrence in the sump and its complex chemistry. The sump simulant solution used in the experiments was an alkaline borate solution (ABS) with or without sodium thiosulfate additive. The composition was chosen to represent the conditions forming during a severe accident where spray solution has accumulated in the bottom of the containment building with a base from pH control and boric acid from spray and possibly RCS. It should be noted that the sump solution in these experiments was extremely simplified and that there would be more components to consider in a real accident scenario. However, the conditions still attempt to represent the actual accident scenario

The experiments were performed by weighing out 30 ± 0.5 mg of tellurium dioxide (Sigma Aldrich) to an 8 ml glass vial before adding 5 ml of either ABS solution either with or without sodium thiosulfate. The ABS solution had 0.23 M H_3BO_3, 0.15 M NaOH and 0.064 M $Na_2S_2O_3$ and the pH of both solutions was around 9. The pH values were determined using a PHM240 pH meter. All samples were prepared in the same way and divided into irradiated and reference samples. The different sample types and changing parameters are presented in Table 7. The nonirradiated reference samples were placed in a heating cabinet at 313 K, while the rest of the samples were placed in Gammacell 220 Co-60 source (MDS Nordion, Atomic Energy of Canada Ltd) for irradiation. The dose rate of the Gammacell 220 was around 5 kGy/h and the maximum dose delivered to the samples was around 1.2 MGy (after 10 days). As the temperature inside the Gammacell220 was approximately 313 K, the reference samples were also kept at this temperature to eliminate the effect of temperature on the results. The samples were exposed to these conditions for a period of time ranging from 1 to 10 days. After taking the samples out, the solid material was allowed to settle at the bottom of the vial, after which the liquid in the samples was filtered with 0.45 μm polyethylene syringe filters (VWR®) and prepared for ICP-MS measurements by diluting with 0.5 M Suprapur® HNO_3 (Merck). The solid material was dried in the heating cabinet and prepared for XRD analysis. All samples were performed in triplicate to obtain statistical significance.

Table 7. Sample types used in the sump experiments.

Sample ID	γ-Irradiated	$Na_2S_2O_3$
TeO_{2_w/o_thio_irrad}	Yes	No
TeO_{2_w/o_thio_ref}	No	No
$TeO_{2\_w/\_thio\_irrad}$	Yes	Yes
$TeO_{2\_w/\_thio\_ref}$	No	Yes

4.3. Analytical methods

Inductively Coupled Plasma Mass Spectrometry, ICP-MS

Tellurium concentration in all of the liquid samples was measured with Inductively Coupled Plasma Mass Spectrometry (Thermo Scientific iCAP Q). The samples were diluted with 0.5 M nitric acid (HNO_3, Sigma Aldrich) containing 1 ppb rhodium as an internal standard (Ultra Scientific). Rhodium was chosen as an internal standard because of its chemical stability. Tellurium standards were prepared from 10 ppm tellurium standard solution in hydrochloric acid (High-Purity Standards). The standards were prepared with concentration ranging from 0 ppb to 100 ppb.

Ion Chromatography

Tellurium speciation was investigated using ion chromatography (IC; Dionex DX-100, IonPac AS4A-SC 4 × 250 mm). The eluant used was a carbonate buffer (conc.). MilliQ water (Millipore) was used as a background sample. The samples were run untreated and undiluted due to the relatively low concentration of tellurium in all of the samples to obtain a detectable signal. Standard solutions were prepared from Na_2TeO_3 (Sigma Aldrich) for Te(IV) and from H_6TeO_6 (Sigma Aldrich) for Te(VI). The samples were compared to the known standards to determine the oxidation state in each sample.

X-Ray Diffraction, XRD

The solid speciation of tellurium precursors from spray experiments as well as the solid material from the sump experiments were investigated with powder X-ray Diffraction (XRD; Siemens D5000 diffractometer with Cu Kα- radiation in case of sump experiment and Bruker D8 Advance with samples obtained from the spray experiments). The samples were ground to a homogeneous consistency before the analysis. Interpretation of the diffractograms was done with DIFFRAC.EVA 4.1.1. (sump) or 5.2. (spray) software using the International Center for Diffraction Data® database.

Instrumental Neutron Activation Analysis, INAA

The tellurium content on the filters and liquid traps obtained from the containment spray experiments was analyzed with Inactive Neutron Activation Analysis (INAA) in Řež Nuclear Research Center in the Czech Republic. The samples were irradiated in an LVR-15 research reactor) with a thermal neutron flux of $2.9 \cdot 10^{13}$ $cm^{-2} \cdot s^{-1}$, epithermal neutron flux of $1.0 \cdot 10^{13}$ $cm^{-2} \cdot s^{-1}$, and fast neutron fluence ($1.0 \cdot 10^{13}$ $cm^{-2} \cdot s^{-1}$). The activity in the irradiated samples was measured with a high-purity germanium (HPGe) detector (Genie 2000, Canberra). The detailed method used in the INAA measurement can be found in Kucera et al.[84].

Electrical Low-Pressure Impactor, ELPI

The mass size distribution of particles was measured online with an Electrical Low Pressure Impactor (Classic ELPI®, Dekati Ltd model 97 2E) with a time resolution of 1 s. Inside the ELPI, particles were charged with a corona charger and then differentiated by their aerodynamic diameter on twelve impaction stages inside the cascade impactor. The number concentration of particles at each impaction stage was derived from the electrical charge of particles and the measured electrical current from the stages, which was mathematically converted to the form of mass concentration data. The inlet of the impactor was approximately at atmospheric pressure and the outlet was at 100 mbar (absolute). The flow rate through ELPI was 9.75 l/min. The measurement range of the ELPI was from approximately 7 nm to 10 μm (less than 5 size channels per decade). The measurement uncertainty was ± 10%. The measurement system was controlled with the ELPIVI software version 4.0 (Dekati Ltd).

Scanning and Transmission Electron Microscopy, SEM/TEM

Particulate aerosol samples were collected during the experiment on 400 mesh carbon film-coated copper grids (Agar Scientific) and analyzed using Scanning or Transmission Electron Microscopy (SEM, TEM). The particulate sampling was performed directly from the gas phase by passing a sample flow of 0.5 l/min through the grid.

The size, morphology, and elemental composition of the collected particles were analyzed using scanning electron microscopy (SEM, Zeiss Crossbeam 540). The elemental analyses in SEM were performed through energy dispersive X-ray analysis (EDX) using Silicon Drift Detectors (SDD, EDAX 30 cm2 Octane Elite™) installed in connection with the SEM. SEM operated at 2 – 3 kV and the probe current was 100 – 200 pA during imaging while EDX spectra were collected using 8 – 10 kV high voltage. The samples with cesium iodide additive were also analyzed by means of TEM (Transmission Electron Microscope, TALOS™ F200X (S)TEM) with 200 kV field emission TEM.

5.   Results and Discussion

The removal efficiency of tellurium species by the containment spray system was investigated in different atmospheric conditions. In addition, the effect of the spray solution composition was also analyzed. The results presented here show the changes in tellurium precursor, particle size distribution and the removal efficiency.

5.2.   Containment spray system

5.2.1. Mass difference

The crucible containing the tellurium precursor was weighed before and after each experiment and the mass differences were used to estimate the release behavior of tellurium under different conditions. The weighing results are presented in Table 8. In Experiments 1-3 performed with TeO_2 in air, the mass decreased 0.20, 0.26 and 0.30 g, respectively, from the initial mass of 1.26 g. Moreover, the volatilization and release were relatively consistent in each condition with a slight increase from dry to humid and humid with CsI. This indicated that humidity and CsI may have an effect on tellurium volatilization and release. However, a conclusion cannot be reached from these results alone due to the relatively small differences in the masses.

In the experiments performed with metallic Te in air, the mass of the precursor decreased 0.05 g in Experiment 4. Moreover, the mass of the tellurium precursor increased 0.009 and 0.070 g in Experiments 5 and 6, respectively. The low decrease or even the slight increase was possibly due to oxidation of metallic tellurium under the experimental conditions. As seen on Figure 8, the color of the precursor (Experiment 5) had changed from black to light grey during the experiment further indicating oxidation of the precursor. This was later analyzed using XRD.

Figure 8. Metallic tellurium precursor before (left) and after (right) Experiment 5.

In Experiments 7–9 with metallic Te under nitrogen atmosphere, the mass decreased significantly during the experiments. In Experiment 7, the mass loss was 0.80 g, which corresponds to 80% of the initial 1.0 g of metallic Te precursor. Experiments 8 and 9 were performed back to back, which made it impossible to determine the mass difference in the individual experiments. However, overall the mass decreased 90% from the initial mass, indicating high overall release.

Table 8. The initial mass of the tellurium precursor and the mass loss observed after each experiment. In Exp. 5 and 6 the negative value indicates mass increase instead of decrease.

Experiment [#]	Duration [min]	Initial Mass [g]	Mass loss [g]
1	190	1.26	0.199
2	151	1.26	0.255
3	171	1.26	0.295
4	186	1.02	0.051[a]
5	182	1.00	-0.009[a]
6	231	1.01	-0.069[a]
7	197	1.00	0.789
8-9[b]	410	1.00	0.883

[a] Tellurium precursor oxidized during the experiment and therefore, the results are not reliable.
[b] Experiments 8 and 9 were performed back to back using the same precursor

5.2.2. Precursor analysis

As previously suggested, the metallic Te precursor may have oxidized when exposed to the oxidizing experimental conditions in Experiments 4–6. This was suggested by the increased mass of the precursor as well as the color change of the precursor from black to light grey. The precursors were therefore analyzed using XRD after the experiments to determine whether the speciation of the solid material had changed during the experiments. The diffractograms for each sample from Experiments 4–6 are presented in Figure 9. All of the precursors after the experiments were found to be mixtures of elemental Te and TeO_2. This is in line with the assumption that Te had oxidized during the experiment, which was also observed from the color change shown in Figure 8. In addition, there were differences in the ratio between Te and TeO_2 between the precursors. Although each sample was found to be a mixture of the two tellurium species, it was observed that the precursor from Experiment 5 (Te in humid air) had more distinctive peaks for metallic Te compared to the precursors from Experiments 4 and 6. This could indicate a lower degree of precursor oxidation, which could be the result of a different behavior of tellurium in humid air compared to dry air or humid air with CsI. However, inconsistent results were also observed with the INAA filter samples as well as the online aerosol measurements. Thus, an error in Experiment 5 cannot be ruled out. It should also be noted that comparing the peak intensities and their ratios is not a straightforward quantification technique, but it can be used for indication purposes.
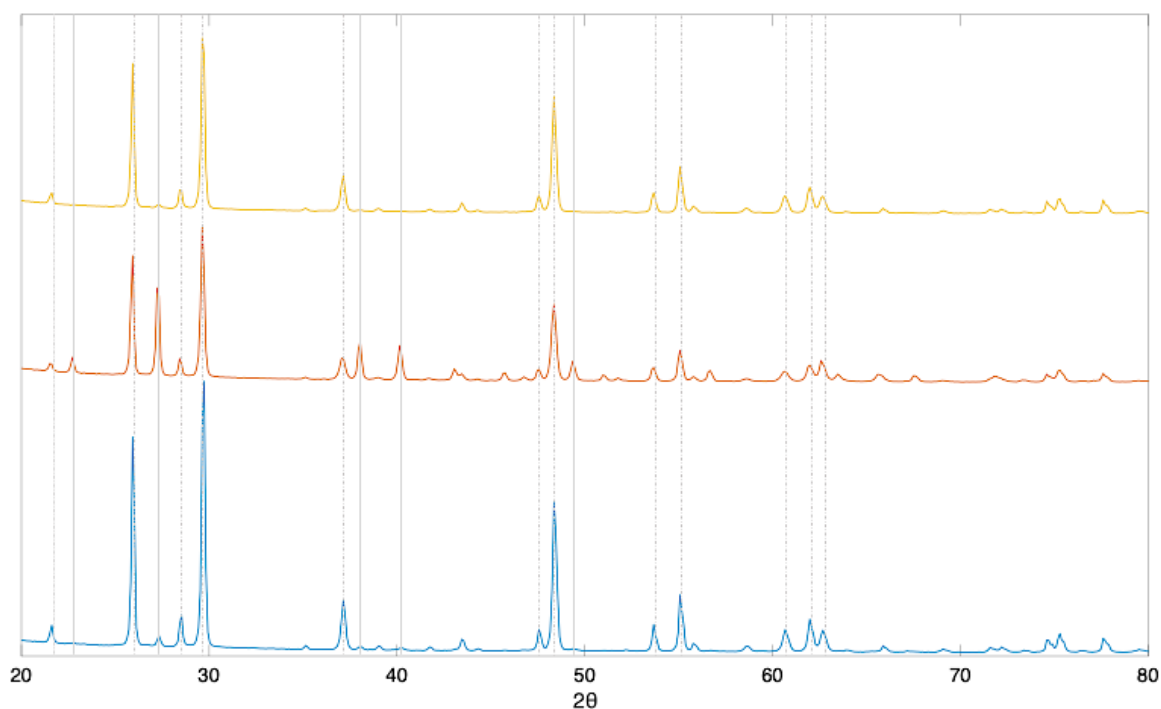
Figure 9. Diffractograms of the precursors from Experiments 4 (bottom), 5 (middle) and 6 (top). The solid lines mark the signals identified for elemental tellurium and the dashed lines the signals for TeO$_2$.

5.2.3. Filter analysis

Some observations regarding the release behavior of tellurium can be made from the reference filter samples taken in the beginning of each experiment without any spray. The filters placed at the end of the system were analyzed with INAA for their tellurium content. The results of the INAA measurements for each experiment are presented in Table 9.

The reference filters from Experiments 1, 2 and 3, where TeO$_2$ was used as a precursor in air, had an increasing tellurium content in the order dry to humid to humid with CsI. This is in line with the literature, which suggests that TeO$_2$ can react with steam to form a more volatile species, possibly TeO(OH)$_2$. However, the speciation during the experiments was not monitored. Thus, the exact reason for the higher volatility cannot be confirmed. The tellurium content on the filter from Experiment 2 with humid air had over twice the amount of tellurium deposition compared to the filter from Experiment 1. Furthermore, the increase from humid air to humid air with CsI had only a slight increase and, taking into account the uncertainties, the results even overlap. It is therefore hard to conclude whether CsI had any significant effect on tellurium release and transport from these results.

26

In Experiments 4, 5 and 6 performed with metallic tellurium in air, there was more fluctuation in the filter results. The filter from Experiment 5 in particular had a very low amount of tellurium deposition compared to Experiments 4 and 6. This result is inconclusive and cannot be explained through literature or other means. As it was already previously mentioned, an experimental error cannot be ruled out when it comes to the low release obtained from Experiment 5.

Finally, the Experiments 7, 8 and 9, where metallic tellurium was used as a precursor in nitrogen atmosphere, the tellurium content on the filter decreased in order of dry to humid to humid with CsI.

Table 9. Filter results for reference filters from spray experiments.

Experiment#	Filter, Te [mg]
1	0.240 ± 0.008
2	0.570 ± 0.018
3	0.588 ± 0.018
4	0.373 ± 0.011
5	0.023 ± 0.0007
6	0.283 ± 0.009
7	0.497 ± 0.015
8	0.348 ± 0.011
9	0.177 ± 0.005

5.2.4. Deposition

As observed in the previous results, the mass of tellurium released from the crucible was significantly higher (excluding Experiments 4–6) than the tellurium content in the filters, traps and sumps combined. In addition, an observation made during the cleanup of the system was that there seemed to be a significant amount of deposition inside the stainless-steel tube leading to the containment unit as well as on the insides of the connectors (Figure 10). This was assumed to be tellurium deposition, most likely TeO_2. However, the deposition was not analyzed further to determine the exact speciation. Tellurium and stainless-steel interactions are relatively well known in the literature[82]. In addition, some severe accident research has shown evidence of tellurium deposition in the RCS[43,83]. It is therefore reasonable to assume that the deposition originates from the released tellurium. However, the amount of deposition was not quantified and thus, the mass balance cannot be fully completed.
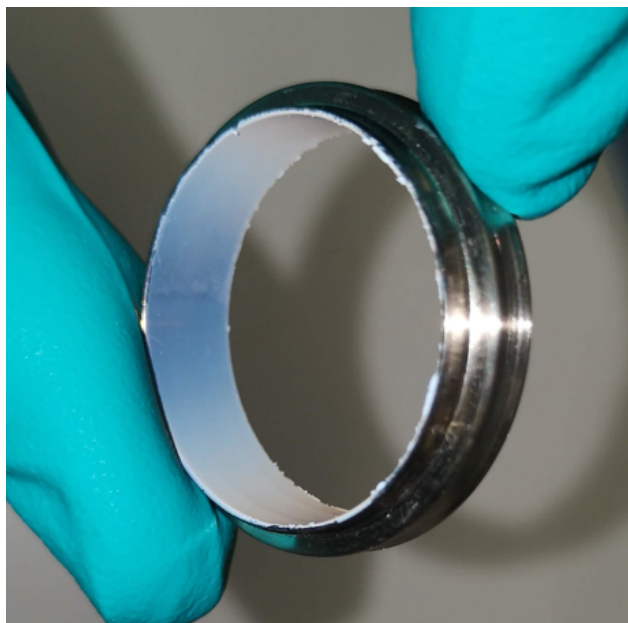
Figure 10. Metallic connector showing the white deposition formed during the experiment.

5.2.5. Particle size distribution

The properties of tellurium aerosols entering the containment unit were monitored online using ELPI. The average mass size distributions describing the aerosol properties inside the spray chamber without spray operation are given in Figure 11. In general, the aerodynamic mass median diameter (AMMD) of tellurium aerosols was less than 1 µm. However, the particles formed large agglomerates, which extended the mass size distribution towards the particle diameters of several µm. The fraction of agglomerates seemed to be more pronounced in the experiments with metallic tellurium precursor (Exp. 4-9). The mass concentration of tellurium aerosol particles varied between the experiments, with the highest concentration was observed in the experiments with TeO_2 precursor. In Experiment 5 (metallic Te precursor in air), the mass concentration was very low and a possible error in the experiment is suspected. The airborne CsI aerosol additive was fed together with tellurium aerosols in Experiments 3, 6 and 9. It seemed that the mass size distribution grew wider due to the CsI particles.
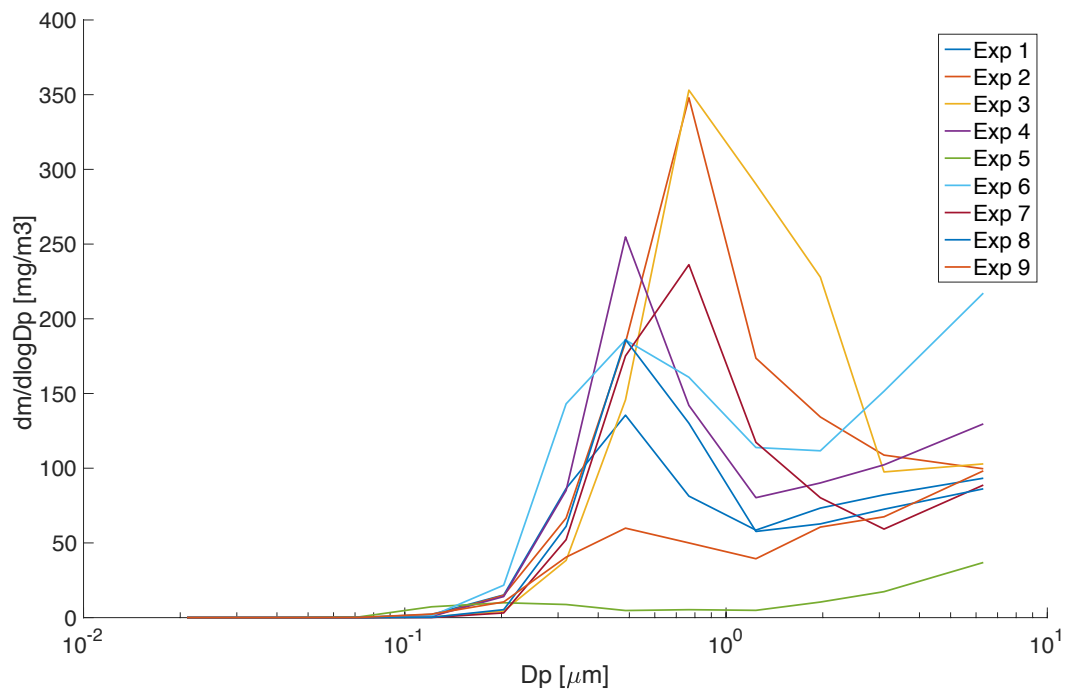

Figure 11. The average mass size distribution of the fed tellurium aerosols in the spray chamber in reference conditions.

5.2.6. Spray removal efficiency

The spray removal efficiencies were calculated from reference and sample filters collected after each experiment. Tellurium content on the filters was analyzed with INAA. The reference filter results as well as the sample filter results from Experiments 1–3, 4–6 and 7–9 are presented in Figures 12, 13 and 14. These were used to calculate the removal efficiencies shown in Table 10. The presented values are not corrected for the actual spray coverage of the spray chamber cross-section – full coverage is assumed now. However, the trends in removal efficiencies between the various experiments can be compared.

Table 10. Removal efficiencies for each spray solution calculated from INAA filter results.

	Removal Efficiency [%]		
Experiment#	**MilliQ water**	**ABS[a] without thiosulfate**	**ABS with thiosulfate**
1	82.5	96.0	96.6
2	87.8	97.0	97.2
3	91.3	97.4	97.3
4	82.8	98.6	98.7
5	73.6	73.1	72.8
6	91.8	98.7	98.8
7	63.0	71.7	74.8
8	70.4	64.5	59.8
9	88.8	92.9	94.4

[a]Alkaline Borate Solution

For Experiments 1-3 where TeO_2 precursor was investigated in air atmosphere, the highest removal efficiencies were obtained with the sprays with higher chemical content. The amount of tellurium on the filters decreased from 240 ug (reference) to 0.001ug and 0.008 ug, corresponding to approximately 97 % removal efficiency for ABS without and with thiosulfate, respectively. MilliQ water spray gave slightly lower efficiency, with tellurium content on the filter being 0.04 ug corresponding to 83 % efficiency.

With metallic tellurium precursor, the removal efficiency varied between the different experimental conditions. In dry air atmosphere, water spray removed 82 % of tellurium species. When the humidity of the air was increased the removal percentage with water decreased to 74 %. With CsI added to the humid air atmosphere, the removal of tellurium species increased again to approximately 92 %. The trend continued with both chemical sprays where removal efficiency was 99% in dry and humid CsI atmospheres, while being around 73% for both chemical sprays in humid air.

In an inert atmosphere (Experiments 7–9), the removal of tellurium species was generally lower compared to the experiments performed in air atmosphere. Tellurium released in dry nitrogen atmosphere was removed with 63, 72 and 75 % efficiency with water, chemical spray without and with sodium thiosulfate, respectively. In contrast, the removal efficiency decreased with increasing chemical composition of the spray solution for tellurium in humid N_2. The percentages were 70, 64, 60 % for water, borate buffer without and with sodium thiosulfate. Finally, the efficiency increased again for Experiment 9 where metallic tellurium was released in humid N_2 with CsI addition. The removal efficiencies were 89-94 % with all three spray solutions.
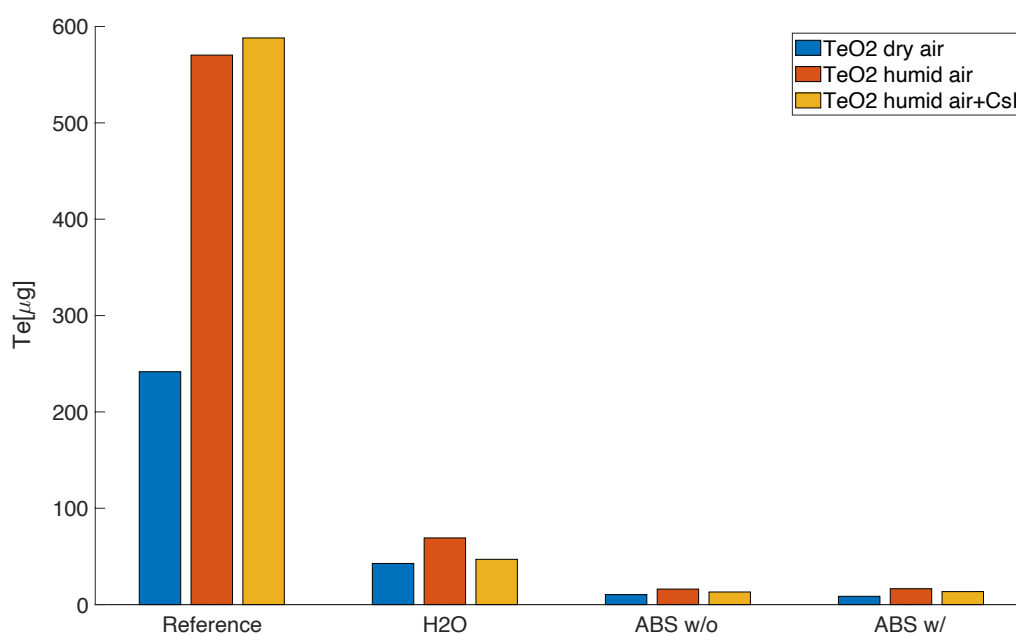
Figure 12. Tellurium dioxide in air atmosphere, Experiments 1 (blue), 2 (orange), 3 yellow).
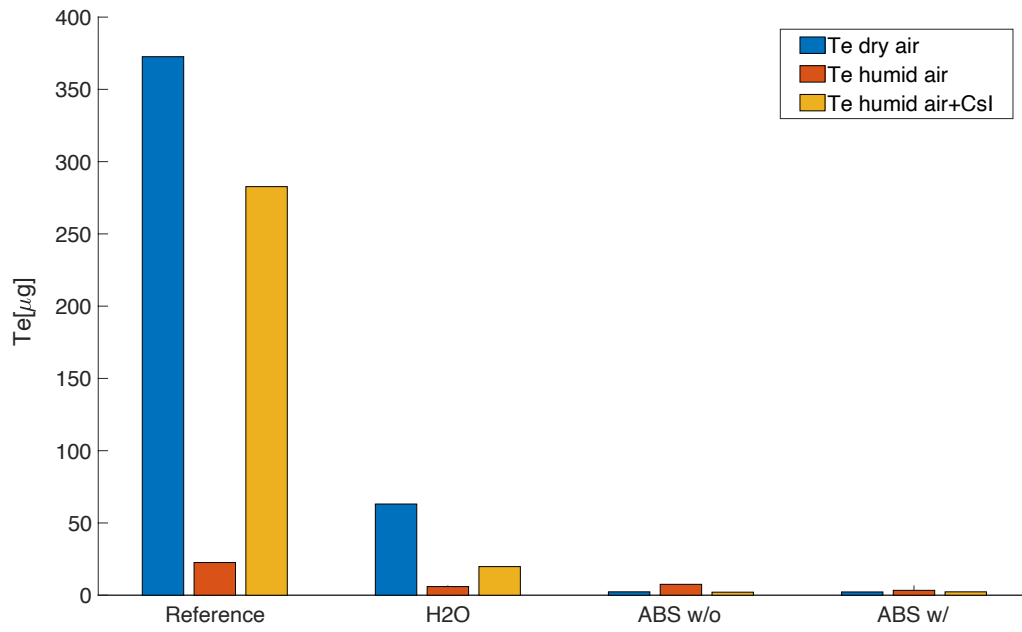
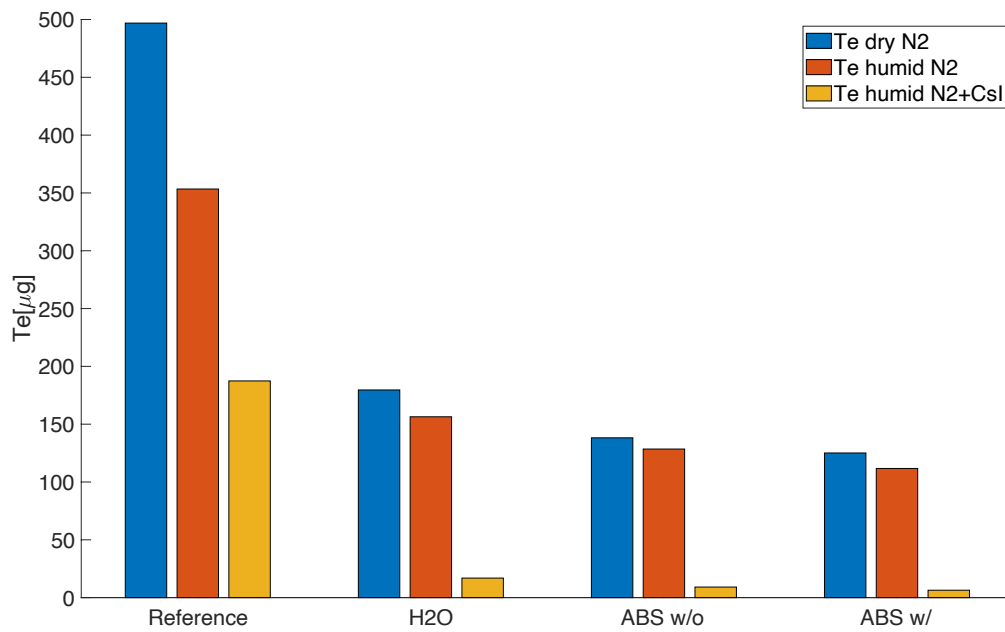*Figure 13. Tellurium in air atmosphere. Experiments 4 (blue), 5 (orange), 6 yellow).*

Figure 14. Tellurium in nitrogen atmosphere. Experiments 7 (blue), 8 (orange), 9 (yellow).

As observed from the results, the efficiency of the CSS was generally relatively high for tellurium species formed under various experimental conditions. One of the main reasons for the high removal is the size of the fed tellurium aerosols which was suitable for the removal (>1μm). In addition, the particle diameter increased slightly when CsI was added to the feed, increasing the removal efficiency even more. However, the removal efficiency was lower in nitrogen atmosphere for the first two spray conditions.

Some observations were also made about the release behavior of elemental Te and TeO_2. It was observed, that metallic Te oxidized partially during the experiments to TeO_2 which decreased the release rate. This is due to the temperature being too low for vaporization of TeO_2. Moreover, there was a significant amount of deposition inside the system. This was not analyzed but is assumed to be TeO_2.

5.3. Tellurium behavior in the containment sump

The behavior of TeO_2 was investigated in alkaline borate solution (ABS) with and without sodium thiosulfate. The results presented below show the TeO_2 behavior in terms of solubility, speciation and redox chemistry.

5.3.1. Solubility of tellurium

The solubility of tellurium dioxide in the simulated sump solution was investigated by measuring the tellurium content in liquid phase. The concentration was measured with ICP-MS and the results are presented in Figure 15 as tellurium concentration as a function of time. The figure shows both irradiated and nonirradiated samples and the time corresponds to either irradiation time or, in the case of the reference samples, the time in the heating cabinet.

In the ABS solution without thiosulfate, the concentration of tellurium increased in the samples with increasing irradiation times. The maximum concentration after 10 days (1.2 MGy) was approximately 26 mM. The corresponding results for the nonirradiated reference sample had a tellurium concentration of 16 mM, which is in line with the values found in literature for TeO_2 solubility[73]. In addition, the reference samples have a consistent concentration after 3 days. It can therefore be assumed that the samples reached an equilibrium. In contrast, the irradiated samples did not reach equilibrium, but the increase in solubility was linear throughout the experiment. The increase indicated a possible change in tellurium speciation to a more soluble form under irradiation. The speciation of tellurium was later investigated with ion chromatography.

The concentration of TeO_2 in the samples in ABS with sodium thiosulfate had a decreasing trend. As shown in Figure 15, the concentration of tellurium decreases with increasing irradiation times, reaching a minimum concentration of 6 mM after 10 days of irradiation. As with the samples without thiosulfate, the concentration did not reach equilibrium but had a linear decrease throughout the experiment. In addition to the decreasing concentration, the color of the solid material changed under irradiation from white to silvery black. This again indicated change in the speciation of the tellurium precursor, possibly to a form of non-soluble elemental tellurium. This was later investigated with XRD. The nonirradiated reference samples exhibited behavior similar to the ones without the thiosulfate additive; solubility reached an equilibrium at around 16 mM and no color change was observed. Moreover, no significant change in pH was observed in any of the samples.

The different behavior between the irradiated and reference samples indicate changes during irradiation. As all of the reference samples reached equilibrium, regardless of the thiosulfate, it is reasonable to assume that the changes in the behavior of TeO_2 were due to water radiolysis products produced by the gamma radiation. Due to the complex chemistry of TeO_2 as well as the fact that the radiolysis of water produces both oxidizing and reducing species, it cannot be

concluded which reactions have taken place without further analysis. However, the increase in solubility indicates a change in speciation to a more soluble species, e.g. Te(VI) in the form of telluric acid, $HTeO_4^-$. Regarding the samples with thiosulfate, the chemistry is more complex. However, the decrease in tellurium concentration and the color change of the solid material indicated a reduction of TeO_2 to metallic Te which is basically a non-soluble species and would therefore also explain the decrease in solubility.
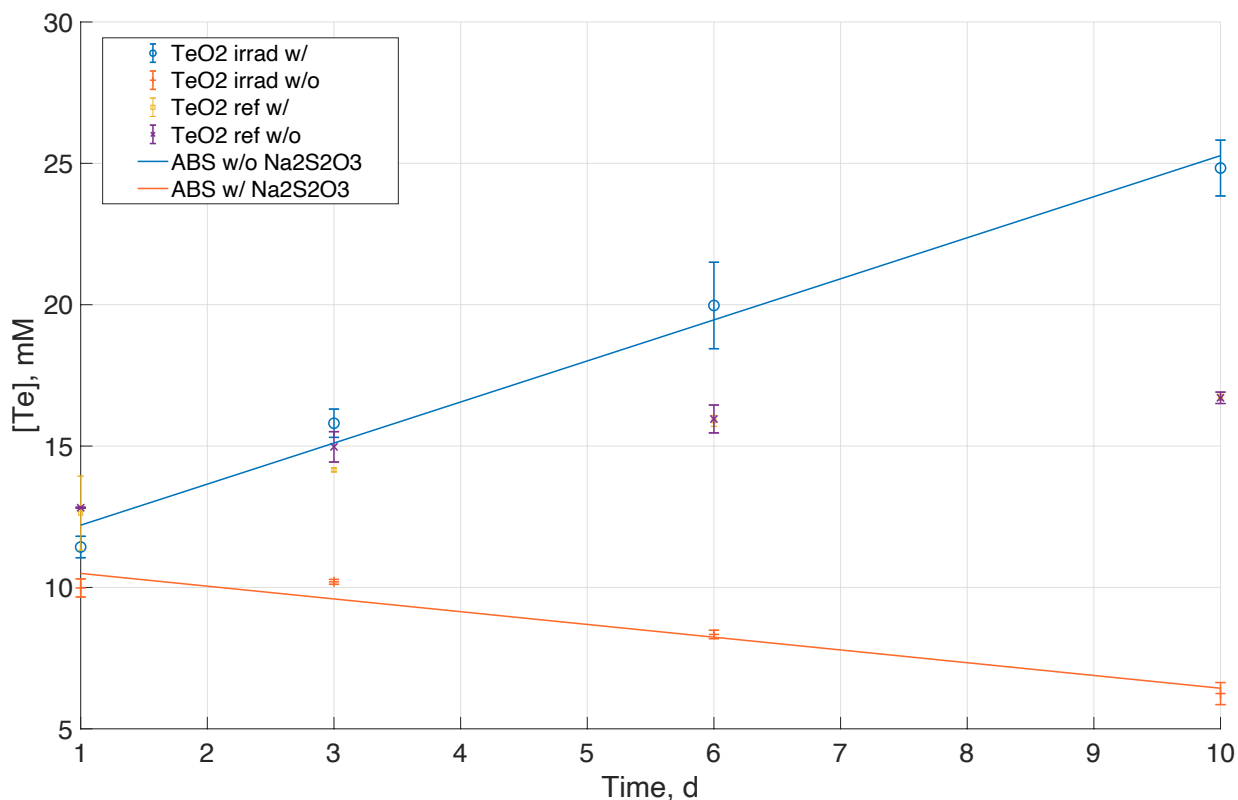
Figure 15. The solubility of tellurium in alkaline borate solution with and without sodium thiosulfate additive. Irradiated and reference samples are all presented. Maximum dose received after 10 days of irradiation was around 1.2 MGy. The solid lines represent the linear trend of the irradiated samples in the two different solutions.

5.3.2. Solid speciation

The speciation of the solid material was investigated with XRD. After the experiment, most of the liquid was removed from the vial and the solid material was dried and ground to homogeneous consistency for XRD analysis. The diffractograms for the irradiated sample in ABS with thiosulfate as well as for the corresponding reference sample are presented in Figure 16. The nonirradiated reference sample was identified as TeO_2, as it was expected. All of the main peaks and their intensities in the diffractogram corresponded to paratellurite TeO_2. The aforementioned color change can also be seen in Figure 15. The solid material in the irradiated sample with thiosulfate was silvery black in color and was identified as a mixture of paratellurite TeO_2 and elemental tellurium Te. The diffractogram of the irradiated sample had the same peaks corresponding to TeO2 but had also signals characteristic to elemental Te. This indicates a reduction of $Te(IV)O_2$ to elemental $Te(0)$ under irradiation in the presence of sodium thiosulfate.
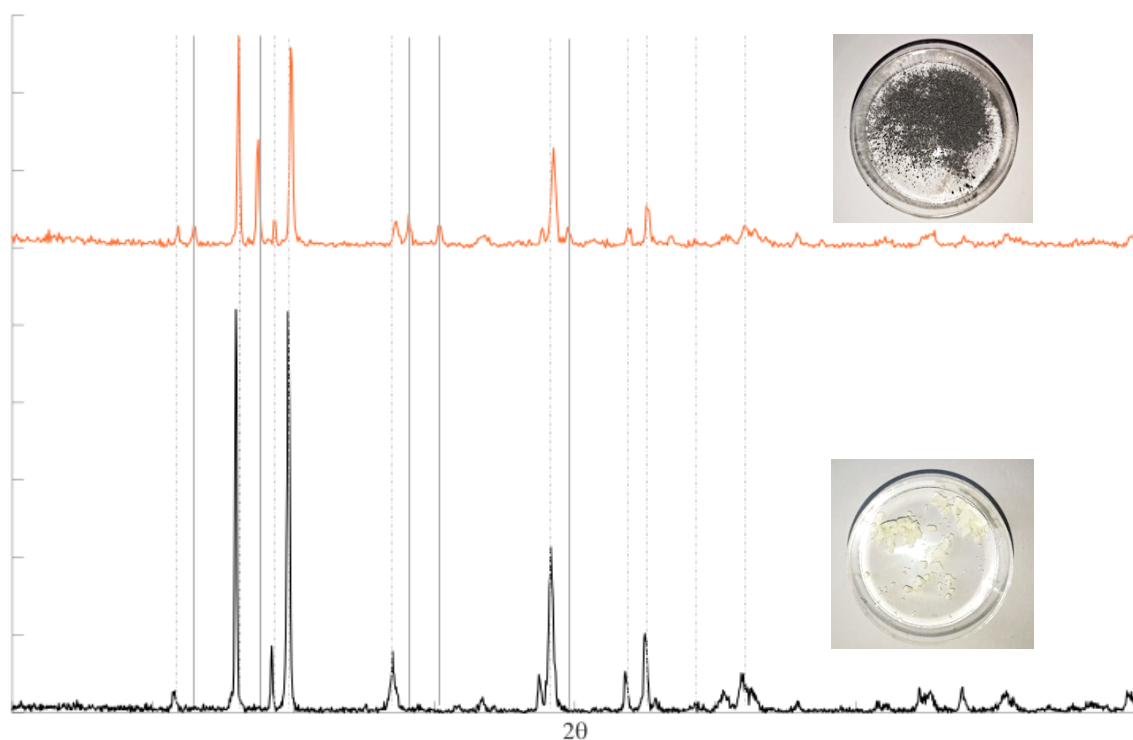

Figure 16. Diffractograms for TeO2 before (bottom) and after (top) irradiation. The solid lines mark the signals identified for elemental tellurium and the dashed lines the signals for TeO2.

5.3.3. Liquid speciation

To determine the changes affecting the solubility of TeO_2 under irradiation, the speciation of tellurium in the simulated sump solution was investigated with ion chromatography (IC). The samples were prepared by filtering the liquid after the experiment. Due to the relatively low concentration of tellurium in all sample, there was no need for dilution. However, this created strong signals for other ions present in the solution in higher concentrations (e.g. borate, OH^-, $S_2O_3^{2-}$, SO_4^{2-}). The aim of the IC analysis was to determine the oxidation state of tellurium by comparing the samples with known standards and using the literature to estimate the prevailing speciation. The results are presented in Figures 17 and 18 for ABS without and with sodium thiosulfate, respectively.

Tellurium was found to be present in two oxidation states, +IV and +VI, depending on the solution and conditions. In the irradiated samples with ABS without thiosulfate, tellurium was present as Te(VI) which forms an anionic complex tellurate, $HTeO_4^-$ in an alkaline solution. The retention time for tellurate was around 6 minutes. The change from Te(IV) to Te(VI) indicated oxidation of tellurium under irradiation. This would also explain the increase in solubility observed in ICP-MS measurements, since the Te(VI) species have significantly higher solubility than $Te(IV)O_2$. Oxidation is most likely due to reactions with the oxidizing water radiolysis products (e.g., H_2O_2, •OH) formed by the gamma radiation.

In the respective reference samples, tellurium was found to exist as $T(IV)O_3^{2-}$ which is expected dissolved species for TeO_2 in alkaline solution. The retention time for Te(IV) complex was also around 6 minutes as for Te(VI). However, the oxidation states could be identified by the shape of the detected peak. For Te(IV), the signal gave a negative peak that was used to indirectly identify the oxidation state. The negative peak was possibly a result of a high positive hydration tendency of the TeO_3^{2-} species resulting in lower conductivity [87]. In contrary, the Te(VI) species had a positive peak with relatively good resolution which made the determination simpler. Although, the retention times were the same, the determination of the exact oxidation state was possible due to the fact that only one or the other species was expected to be present in each sample. The standards were prepared in a manner similar to that of the samples, which validated the identification.

In the samples containing $Na_2S_2O_3$, Te was found to be present as $Te(IV)O_3^{2-}$ in both irradiated and reference samples. Moreover, this indicated no change in the dissolved species under irradiation.
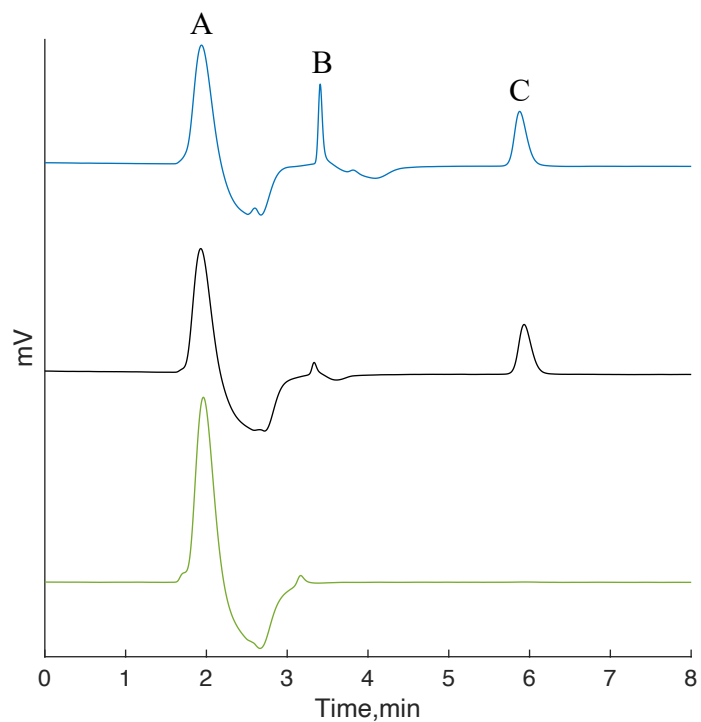
Figure 17. Ion chromatograms for alkaline borate solution standard (bottom), Te(VI) standard in ABS (middle) and TeO$_2$ irradiated in ABS (top). The peaks correspond to A: OH$^-$, B: Borate C: Te(VI)
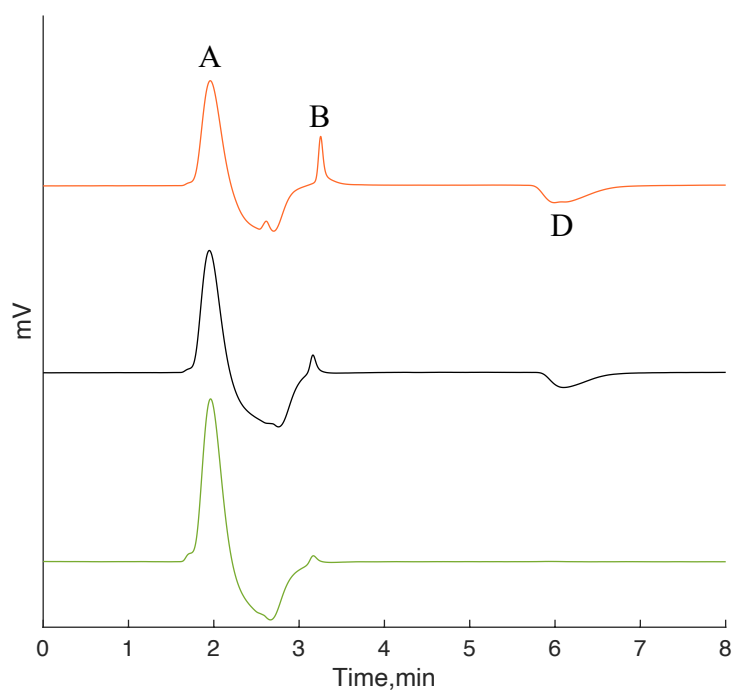

Figure 18. Ion chromatograms for alkaline borate solution standard (bottom), Te(IV) standard in ABS, TeO$_2$ irradiated in ABS with thiosulfate. The peaks correspond to A: OH$^-$, B: Borate D: Te(IV)

IC was also used to analyze the changes in speciation in the simulated sump solution. To further investigate the effect of irradiation on the solution matrix, the simulated sump solution was irradiated without TeO_2. The solution was analyzed with IC before and after irradiation and the chromatograms are presented in Figure 19. Before irradiation, the chromatogram had characteristic peaks for OH^-, and $S_2O_3^{2-}$ at around 12 and 34 minutes, respectively. After irradiation, the $S_2O_3^{2-}$ peak had disappeared and SO_4^{2-} was instead present, indicating oxidation of sulfur under irradiation. This has already been suggested in literature in previous studies[88]. Moreover, the chromatogram had more species with short retention times after irradiation. This is possible due to changes in boron speciation and possible formation of different polyborates. However, the determination of the exact speciation was not possible and requires further investigation.
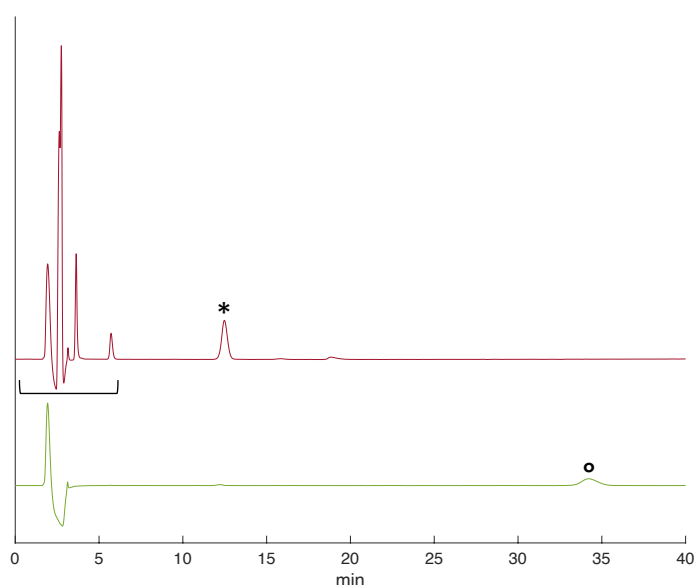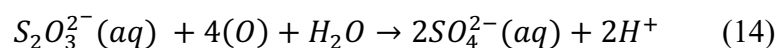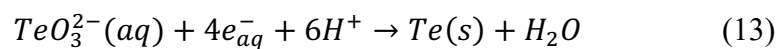

Figure 19. Ion chromatograms for non-irradiated (bottom) and irradiated (top) ABS with thiosulfate. The suspected change in borate speciation is seen on the top chromatogram at around 2-6 min and the sulfate (*) and thiosulfate (°) signal are also marked

39

As it was observed from all of the different analysis methods, there was evidence of changes in tellurium, thiosulfate and possibly borate speciation. Tellurium was found to oxidize from tellurite(IV) to tellurate(VI) in the alkaline borate solution without sodium thiosulfate. This oxidation can also explain the increase in the tellurium concentration with longer irradiation times observed in the ICP-MS measurement due to the fact that Te(VI) is more soluble in aqueous solutions than Te(IV). The oxidation is most likely a result of tellurite reacting with the oxidizing water radiolysis products produced by the ionizing radiation. A possible reaction for the oxidation is presented in Reaction 12. However, it should be noted that it is not possible to differentiate whether tellurite reacts with H_2O_2 or OH radicals. It is most likely a combination of both reactions.

$$TeO_3^{2-}(aq) + H_2O_2 \rightarrow \ HTeO_4^-(aq) + OH^- \qquad (12)$$
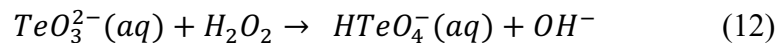
According to the results obtained from XRD measurements of the solid material after the experiment in alkaline borate solution with thiosulfate, there is clear indication of tellurium reduction from Te(IV)O_2 to elemental Te. In addition, the IC analysis of the solution before and after irradiation showed the oxidation of thiosulfate to sulfate. By combining these two observations, it is suggested that there are two separate reactions taking place in the system under irradiation; tellurite(IV) reduction by the reducing radiolysis products (Reaction 13) and thiosulfate reaction with the oxidizing water radiolysis products (Reaction 14). This is supported by literature that suggest that thiosulfate is a relatively strong oxidizing radical scavenger[89,90]. As demonstrated earlier, in the presence of both, oxidizing and reducing radiolysis products, TeO_3^{2-} has tendency to preferentially oxidize. The reason for this is due to the difference in the electrode potentials. The potential for oxidation reaction from TeO_3^{2-} to $HTe(VI)O_4^-$ is smaller than that of the reduction from TeO_3^{2-} to elemental tellurium (Table 4). Therefore, it is more favorable to follow the oxidative path. However, the number of oxidizing products is limited in the presence of thiosulfate. This means that only reducing products are readily available to react with.

$$TeO_3^{2-}(aq) + 4e_{aq}^- + 6H^+ \rightarrow Te(s) + H_2O \qquad (13)$$

$$S_2O_3^{2-}(aq) + 4(O) + H_2O \rightarrow 2SO_4^{2-}(aq) + 2H^+ \qquad (14)$$

6. Conclusions

This work investigated the behavior of tellurium in terms of containment spray system efficiency as well as the behavior of tellurium dioxide in the containment sump. The results obtained here may contribute to improved modeling of the tellurium source term. Furthermore, the results improve knowledge about the behavior and management of tellurium species under severe accident conditions.

In terms of the containment spray system efficiency, it was found that the spray is relatively effective in removing tellurium species formed under various conditions. Higher removal efficiencies were obtained using chemical spray solutions instead of water. However, water spray removed at least 63 % of all tellurium species. In most experiments, the efficiency was even higher. Results obtained from the experiments with metallic tellurium in humid air atmosphere were inconsistent with the other experiments. The release was very low compared to the other conditions. Experimental error can therefore not be ruled out. Moreover, the effect of cesium iodide was also investigated at it was found to increase the removal efficiency. This was most likely due to agglomeration of aerosols to larger particles. However, there was a larger increase when adding CsI to the feed in experiments performed in nitrogen atmosphere which should be further investigated.

The containment sump chemistry was found to have an effect on tellurium solubility and speciation. Results show that tellurium dioxide solubility increased in alkaline borate solution under irradiation. This was due to oxidation of tellurium dioxide to more soluble telluric acid species. When the alkaline borate solution had sodium thiosulfate added to it, the solubility of tellurium dioxide decreased under irradiation. In addition, the excess solid tellurium dioxide precursor reduced to elemental tellurium. This is suspected to be due to thiosulfate ions scavenging the oxidizing water radiolysis product, leaving the reducing product readily available. Due to the complex redox chemistry of TeO_2, both oxidation and reduction reactions are possible. Therefore, it can be concluded from the results that either oxidation or reduction occurred in the two different sump conditions. These results raise a question as to whether the increase in tellurium solubility could be important in terms of possible reactions between tellurium and other fission products in the sump. These reactions could further lead to formation of volatile species and therefore affect the source term estimations.

Future work

The tellurium source term is still lacking information in terms of the possible formation and behavior of organic tellurides. Although this has been suggested previously, there is no relevant experimental data to found in literature. In addition, the ion chromatogram indicated that borate might react under irradiation and change its speciation. This might be of interest in future work.

The possible reactions between telluric acid and other fission products, e.g. iodine, is also of interest in future work. Being an oxidizing agent, telluric acid could potentially react with dissolved iodide and oxidize it to a volatile form.

Acknowledgements

References

1. IEA, "World Energy Balances: Overview," IEA, Paris, (2020); https://www.iea.org/reports/world-energy-balances-overview.
2. B. K. SOVACOOL, "The costs of failure: A preliminary assessment of major energy accidents, 1907-2007," Energy Policy **36** 5, 1802, Elsevier (2008); https://doi.org/10.1016/j.enpol.2008.01.040.
3. NEA/OECD, "Chernobyl: Assessment of Radiological and Health Impacts," (2002).
4. WORLD HEALTH ORGANZATION, "Chernobyl: The true scale of the accident 20 years later a UN report provides definitive answers and ways to repair lives," International Atomic Energy Agency (IAEA) (2005).
5. A. HASEGAWA et al., "Emergency Responses and Health Consequences after the Fukushima Accident; Evacuation and Relocation," Clin. Oncol. **28** 4, 237, Elsevier Ltd (2016); https://doi.org/10.1016/j.clon.2016.01.002.
6. B. W. BROOK et al., "Why nuclear energy is sustainable and has to be part of the energy mix," Sustain. Mater. Technol. **1**, 8, Elsevier (2014); https://doi.org/10.1016/j.susmat.2014.11.001.
7. P. A. KHARECHA and J. E. HANSEN, "Prevented mortality and greenhouse gas emissions from historical and projected nuclear power," Environ. Sci. Technol. **47** 9, 4889, UTC (2013); https://doi.org/10.1021/es3051197.
8. J. ROBBINS and A. B. SCHNEIDER, "Thyroid Cancer Following Exposure to Radioactive Iodine," Kluwer Academic Publishers (2000).
9. INTERNATIONAL ATOMIC ENERGY AGENCY, "The International Nuclear and Radiological Event Scale User's Manual" (2008).
10. S. Y. F. CHU, L. P. EKSRÖM, and R. B. FIRESTONE, "Decay Data Search;" 1999; http://nucleardata.nuclear.lu.se/toi/; (current as of Sep. 4, 2020).
11. M. DREICER et al., "Consequences of the Chernobyl accident for the natural and human environments. No. UCRL-JC-125028; CONF-960404-3. Lawrence Livermore National Lab., CA (United States), (1996).
12. A. STOHL, P. SEIBERT, and G. WOTAWA, "The total release of xenon-133 from the Fukushima Dai-ichi nuclear power plant accident," J. Environ. Radioact. **112**, 155, Elsevier (2012); https://doi.org/10.1016/j.jenvrad.2012.06.001.
13. UNSCEAR, "SOURCES AND EFFECTS OF IONIZING RADIATION (annex D)," United Nations, New York (2008).
14. M. CHINO et al., "Preliminary estimation of release amounts of 131i and 137cs accidentally discharged from the fukushima daiichi nuclear power plant into the atmosphere," J. Nucl. Sci. Technol. **48** 7, 1129 (2011); https://doi.org/10.1080/18811248.2011.9711799.
15. G. STEINHAUSER, A. BRANDL, and T. E. JOHNSON, "Comparison of the Chernobyl and Fukushima nuclear accidents: A review of the environmental impacts," Sci. Total Environ. **470**–**471**, 800, Elsevier (2014); https://doi.org/10.1016/J.SCITOTENV.2013.10.029.
16. NEA/OECD, "Nuclear Fuel Behaviour Under Reactivity-initiated Accident (RIA) Conditions State-of-the-art Report," (2010).

17. INTERNATIONAL ATOMIC ENERGY AGENCY, "INSAG-7: The Chernobyl Accident - Updating of INSAG-1" (1992).

18. V. D. KURINY et al., "Particle-associated Chernobyl fall-out in the local and intermediate zones," Ann. Nucl. Energy **20** 6, 415, Pergamon (1993); https://doi.org/10.1016/0306-4549(93)90067-Y.

19. H. HIGUCHI et al., "Radioactivity in surface air and precipitation in Japan after the Chernobyl accident," J. Environ. Radioact. **6** 2, 131, Elsevier (1988); https://doi.org/10.1016/0265-931X(88)90056-2.

20. P.H. GUDIKSEN, T.F. HARVEY, R. LANGE, "Chernobyl source term, atmospheric dispersion, and dose estimation" No. UCRL-98235; CONF-880367-3. Lawrence Livermore National Lab., CA (USA), (1988).

21. P. ANTTILA, M. KULMALA, and T. RAUNEMAA, "Dry and wet deposition of chernobyl aerosols in Southern Finland," J. Aerosol Sci. **18** 6, 939, Pergamon (1987); https://doi.org/10.1016/0021-8502(87)90161-3.

22. U. BALTENSPERGER et al., "Chernobyl radioactivity in size-fractionated aerosol," J. Aerosol Sci. **18** 6, 685, Pergamon (1987); https://doi.org/10.1016/0021-8502(87)90097-8.

23. J. TSCHIERSCH and B. GEORGI, "Chernobyl fallout size distribution in Urban areas," J. Aerosol Sci. **18** 6, 689, Pergamon (1987); https://doi.org/10.1016/0021-8502(87)90098-X.

24. S. SALMINEN-PAATERO et al., "Nuclear contamination sources in surface air of Finnish Lapland in 1965–2011 studied by means of 137Cs, 90Sr, and total beta activity," Environ. Sci. Pollut. Res. **26** 21, 21511, Springer Verlag (2019); https://doi.org/10.1007/s11356-019-05451-0.

25. S. ALMGREN and M. ISAKSSON, "Vertical migration studies of 137Cs from nuclear weapons fallout and the Chernobyl accident," J. Environ. Radioact. **91** 1–2, 90, Elsevier (2006); https://doi.org/10.1016/j.jenvrad.2006.08.008.

26. INTERNATIONAL ATOMIC ENERGY AGENCY (IAEA), "The Fukushima Daiichi Accident: Technical Volume 1/5, Description and Context of the Accident" (2015).

27. K. HIROSE, "2011 Fukushima Dai-ichi nuclear power plant accident: Summary of regional radioactive deposition monitoring results," J. Environ. Radioact. **111**, 13, Elsevier (2012); https://doi.org/10.1016/j.jenvrad.2011.09.003.

28. R. QUERFELD et al., "Radionuclides in surface waters around the damaged Fukushima Daiichi NPP one month after the accident: Evidence of significant tritium release into the environment," Sci. Total Environ. **689**, 451, Elsevier B.V. (2019); https://doi.org/10.1016/j.scitotenv.2019.06.362.

29. M. CHINO et al., "Preliminary estimation of release amounts of 131i and 137cs accidentally discharged from the fukushima daiichi nuclear power plant into the atmosphere," J. Nucl. Sci. Technol. **48** 7, 1129 (2011); https://doi.org/10.1080/18811248.2011.9711799.

30. R. PERIÁÑEZ, K. S. SUH, and B. Il MIN, "Local scale marine modelling of Fukushima releases. Assessment of water and sediment contamination and sensitivity to water circulation description," Mar. Pollut. Bull. **64** 11, 2333, Pergamon (2012); https://doi.org/10.1016/j.marpolbul.2012.08.030.

31.   T. CHRISTOUDIAS and J. LELIEVELD, "Modelling the global atmospheric transport and deposition of radionuclides from the Fukushima Dai-ichi nuclear accident," Atmos. Chem. Phys. **13** 3, 1425 (2013); https://doi.org/10.5194/acp-13-1425-2013.

32.   N. YOSHIDA and J. KANDA, ""Tracking the Fukushima radionuclides."Science **336**, no. 6085. p.1115-1116, (2012).

33.   K. TAGAMI et al., "Estimation of Te-132 Distribution in Fukushima Prefecture at the Early Stage of the Fukushima Daiichi Nuclear Power Plant Reactor Failures" (2013); https://doi.org/10.1021/es304730b.

34.   N. KINOSHITA et al., "Assessment of individual radionuclide distributions from the Fukushima nuclear accident covering central-east Japan," Proc. Natl. Acad. Sci. U. S. A. **108** 49, 19526 (2011); https://doi.org/10.1073/pnas.1111724108.

35.   K. SAITO et al., "Detailed deposition density maps constructed by large-scale soil sampling for gamma-ray emitting radioactive nuclides from the Fukushima Dai-ichi Nuclear Power Plant accident," J. Environ. Radioact. (2015); https://doi.org/10.1016/j.jenvrad.2014.02.014.

36.   S. TAKAHASHI et al., "Estimation of the Release Time of Radio-Tellurium During the Fukushima Daiichi Nuclear Power Plant Accident and Its Relationship to Individual Plant Events," Nucl. Technol. **205** 5, 646 (2018); https://doi.org/10.1080/00295450.2018.1521186.

37.   K. NISHIHARA, K AND IWAMOTO, H AND SUYAMA, "Estimation of fuel compositions in Fukushima-Daiichi Nuclear Power Plant. JAEA-Data/Code 2012-018 (2012)" (2012).

38.   Y. PONTILLON, G. DUCROS, and P. P. MALGOUYRES, "Behaviour of fission products under severe PWR accident conditions VERCORS experimental programme - Part 1: General description of the programme," Nucl. Eng. Des. **240** 7, 1843, Elsevier Ltd (2010); https://doi.org/10.1016/j.nucengdes.2009.06.028.

39.   P. MARCH and B. SIMONDI-TEISSEIRE, "Overview of the facility and experiments performed in Phébus FP," Ann. Nucl. Energy **61**, 11, Pergamon (2013); https://doi.org/10.1016/J.ANUCENE.2013.03.040.

40.   R. DE BOER and E. H. P. CORDFUNKE, "The chemical form of fission product tellurium during reactor accident conditions," J. Nucl. Mater. **240** 2, 124, Elsevier (1997); https://doi.org/10.1016/S0022-3115(96)00600-9.

41.   R. DE BOER and E. H. P. CORDFUNKE, "Reaction of tellurium with Zircaloy-4," J. Nucl. Mater. **223** 2, 103, North-Holland (1995); https://doi.org/10.1016/0022-3115(95)00005-4.

42.   J. ESPEGREN, F., KÄRKELÄ, PASI, A.E., TAPPER, U., KUCERA, J., LERUM, V.L., OMTVEDT and C. EKBERG, "Tellurium Transport in the RCS under conditions relevant for severe nuclear accidents."(2020). Manuscript submitted for publication

43.   C. GONZÁLEZ and A. ALONSO, "The kinetics of the reactions of tellurium with stainless steel surfaces and silver aerosols," Nucl. Eng. Des. **180** 1, 1, Elsevier BV (1998); https://doi.org/10.1016/S0029-5493(97)00293-8.

44.   M. LAURIE et al., "Containment behaviour in Phébus FP," Ann. Nucl. Energy **60**, 15, Pergamon (2013); https://doi.org/10.1016/J.ANUCENE.2013.03.032.

45. B. R. SEHGAL, Nuclear safety in light water reactors: severe accident phenomenology, Academic Press (2011).

46. L. SOFFER et al., "Accident Source Terms for Light-Water Nuclear Power Plants Final Report" (1995).

47. B. W. SPENCER et al., "Investigation of molten corium-concrete interaction phenomena and aerosol release. " No. CONF-870816-27. Argonne National Lab., IL (USA); Electric Power Research Inst., Palo Alto, CA (USA), (1987).

48. G. CENERINO, E.H.P. CORDFUNKE, and M.E. HUNTERLAAR, "Fission product release during MCCI. CEC nuclear safety program: MCCI project." No. ECN-RX--95-003. Netherlands Energy Research Foundation (ECN), (1995)

49. S. HERMSMEYER et al., "Review of current Severe Accident Management (SAM) approaches for Nuclear Power Plants in Europe requirements" (2014); https://doi.org/10.2790/38824.

50. C. B. ASHMORE, J. R. GWYTHER, and H. E. SIMS, "Some effects of pH on inorganic iodine volatility in containment," Nucl. Eng. Des. **166** 3, 347, North-Holland (1996); https://doi.org/10.1016/S0029-5493(96)01252-6.

51. CSNI, "Insights into the control of the release of iodine, cesium, strontium and other fission products in the containment by severe accident management." NEA/OECD, Paris (2000).

52. R. K. HILLIARD et al., "Removal of Iodine and Particles by Sprays in the Containment Systems Experiment," Nucl. Technol. **10** 4, 499 (1971); https://doi.org/10.13182/nt71-a16261.

53. K-H. NEEB, The radiochemistry of nuclear power plants with light water reactors. Walter de Gruyter, (2011); https://doi.org/10.1515/9783110812015.

54. L.F. PARSLY, "Spray Program at the Nuclear Safety Pilot Plant." Nucl. Technol. **10** 4, 472 (1971); https://doi.org/10.13182/nt71-a16259.

55. W. E. JOYCE, "Sodium Thiosulfate Spray System for Radioiodine Removal," Nucl. Technol. **10** 4, 444 (1971); https://doi.org/10.13182/NT71-A16254.

56. T. LAVONEN, "Chemical effects in the sump water pool during post-LOCA conditions-literature review" (2013).

57. C. B. BAHN, "Chemical effects on PWR sump strainer blockage after a loss-of-coolant accident: Review on U.S. research efforts," Nucl. Eng. Technol. (2013); https://doi.org/10.5516/NET.07.2013.705.

58. M. AGRELL et al., "Update Knowledge Base for Long-term Core Cooling Reliability." No. NEA-CSNI-R--2013-12. NEA/OECD (2013).

59. R. SANDRINE et al., "Precipitate formation contributing to sump screens clogging of a nuclear power plant during an accident," Chem. Eng. Res. Des. **86** 6, 633, Elsevier (2008); https://doi.org/10.1016/J.CHERD.2008.03.016.

60. A. AUVINEN, R. ZILLIACUS, and J. JOKINIEMI, "Chlorine release from hypalon cable insulation during severe nuclear reactor accidents," Nucl. Technol. **149** 2, 232 (2005); https://doi.org/10.13182/NT05-A3592.

61. J. MCFARLANE, "Fission product tellurium chemistry from fuel to containment." No. PSI--97-02.(1996).

62.   B.R. BOWSHER, S. DICKINSON, A.L. NICHOLS, R.A. GOMME and J.S.OGDEN, "Chemical forms of fission product tellurium in a severe reactor accident," Am. Chem. Soc. Div. Nucl. Chem. Technol. **192** (1986).

63.   E. C. BEAHM, "Tellurium Behavior in Containment under Light Water Reactor Accident Conditions," Nucl. Technol. **78** 3, 295, Taylor & Francis (1987); https://doi.org/10.13182/NT87-A15995.

64.   S. GUENTAY et al., "Radiochemical studies of the retention of volatile iodine in aqueous solutions," J. Radioanal. Nucl. Chem. **273** 3, 557 (2007); https://doi.org/10.1007/s10967-007-0909-3.

65.   W. H. HAMILL, "A model for the radiolysis of water," J. Phys. Chem. **73** 5, 1341 (1969); https://doi.org/10.1021/j100725a027.

66.   B. J. MINCHER et al., "Radiation chemistry and the nuclear fuel cycle," J. Radioanal. Nucl. Chem. **282** 2, 645, Springer Netherlands (2009); https://doi.org/10.1007/s10967-009-0156-x.

67.   W. G. BURNS and H. E. SIMS, "Effect of radiation type in water radiolysis," J. Chem. Soc. Faraday Trans. 1 Phys. Chem. Condens. Phases **77** 11, 2803 (1981); https://doi.org/10.1039/F19817702803.

68.   C. FERRADINI and J. P. JAY-GERIN, "Effect of pH on water radiolysis: a still open question - a minireview," Res. Chem. Intermed. **26** 6, 549 (2000); https://doi.org/10.1163/156856700X00525.

69.   D. SWIATLA-WOJCIK, "Computation of the effect of pH on spur chemistry in water radiolysis at elevated temperatures," Nukleonika **Vol. 53**, **s**, 31 (2008).

70.   N. BELZILE and Y.-W. CHEN, "Tellurium in the environment: A critical review focused on natural waters, soils, sediments and airborne particles," Appl. Geochemistry **63**, 83, Pergamon (2015); https://doi.org/10.1016/J.APGEOCHEM.2015.07.002.

71.   D. C. MCPHAIL, "Thermodynamic properties of aqueous tellurium species between 25 and 350°C," Geochim. Cosmochim. Acta **59** 5, 851 (1995); https://doi.org/10.1016/0016-7037(94)00353-X.

72.   M. BOUROUSHIAN, "Electrochemistry of metal chalcogenides.", Springer Science & Business Media. (2010).

73.   M. POURBAIX, "Atlas of electrochemical equilibria in aqueous solutions.", Oxford, New York, Pergamon Press (1966).

74.   A. HABERSBERGEROVÁ and B. BARTONÍČEK, "Radiolysis of iodine compounds in model systems of PWR," Radiat. Phys. Chem. **21** 3, 289 (1983); https://doi.org/10.1016/0146-5724(83)90157-7.

75.   S. IMOTO and T. TANABE, "Chemical state of tellurium in a degraded LWR core" Journal of Nuclear Materials 154, no. 1, p. 62-66. (1988).

76.   J. MCFARLANE and J. C. LEBLANC, "Fission-product tellurium and cesium telluride chemistry revisited. " No. AECL--11333. Atomic Energy of Canada Ltd., (1996).

77.   J. L. COLLINS, M. F. OSBORNE, and R. A. LORENZ, "Fission Product Tellurium Release Behavior Under Severe Light Water Reactor Accident Conditions," Nucl. Technol. **77** 1, 18, Taylor & Francis (1987); https://doi.org/10.13182/NT87-A33948.

78.   B. R. BOWSHER, "Fission-product chemistry and aerosol behaviour in the primary circuit of a pressurized water reactor under severe accident conditions," Prog. Nucl. Energy **20** 3, 199, Pergamon (1987); https://doi.org/10.1016/0149-1970(87)90006-0.

79.   F. GARISTO, "Thermodynamics of iodine, cesium and tellurium in the primary heat-transport system under accident conditions." No. AECL--7782. Atomic Energy of Canada Ltd., (1982).

80.   A. P. MALINAUSKAS et al., "The Interaction of Tellurium Dioxide and Water Vapor," Nucl. Appl. Technol. **8** 1, 52 (1970); https://doi.org/10.13182/NT70-A28633.

81.   R. S. DICKSON and G. A. GLOWA, "Tellurium behaviour in the Fukushima Dai-ichi Nuclear Power Plant accident," in Journal of Environmental Radioactivity (2019); https://doi.org/10.1016/j.jenvrad.2019.03.024.

82.   C. MILLER, DM AND WINKLER, "The measurement of the absolute rates of removal of lead and tellurium mirror by a free radical stream," Can. J. Chem. **29** 7, 537 (1951).

83.   W.A. HERRMANN (ed.), "Synthetic Methods of Organometallic and Inorganic Chemistry, vol. 4 (1997)", Georg Thieme Verlag, Stuttgart (2014); https://doi.org/10.1055/b-003-108605.

84.   J. KUČERA et al., "Tellurium determination by three modes of instrumental neutron activation analysis in aerosol filters and trap solutions for the simulation of a severe nuclear accident," Microchem. J. **158**, 105139, Elsevier Inc. (2020); https://doi.org/10.1016/j.microc.2020.105139.

85.   R. A. SALLACH, C. J. GREENHOLT, and A. R. TAIG, "Chemical interactions of tellurium vapors with reactor materials", No. NUREG/CR--2921. Sandia National Labs., (1984).

86.   G. LE MAROIS, M. MEGNIN, "Assessment of fission product deposits in the reactor coolant system: the DEVAP program," Nucl. Saf. **35** 2, 213 (1994).

87.   L. T. VLAEV and V. G. GEORGIEVA, "Activation Energy for Electroconduction of Aqueous Solutions of Sulfuric and Selenic Acids and Potassium Tellurate," Russ. J. Electrochem. **40** 6, 674 (2004); https://doi.org/10.1023/B:RUEL.0000032021.43984.d3.

88.   W. N. BISHOP and D. A. NITTI, "Stability of Thiosulfate Spray Solutions," Nucl. Technol. **10** 4, 449 (1971); https://doi.org/10.13182/NT71-A16255.

89.   M. CABRINI, S. LORENZI, and T. PASTORE, "Effects of thiosulfates and sulphite ions on steel corrosion," Corros. Sci. **135**, 158, Elsevier Ltd (2018); https://doi.org/10.1016/j.corsci.2018.02.046.

90.   R. K. ULRICH, G. T. ROCHELLE, and R. E. PRADAS, "Enhanced oxygen absorption into bisulphite solutions containing transition metal ion catalysts. " Chemical engineering science 41, no. 8, p. 2183-2191, (1986).